# 11. Flow with Heat Transfer

We now turn to one-dimensional steady flow with heating or cooling. Our development will follow a familiar pattern from isentropic flow and frictional flow: we will examine differential relations to see how flow responds to heating and cooling, and then develop integral relations that apply to a finite control volume and that utilize the reference state of the flow at sonic conditions. Finally, we will consider the possible scenarios when heating and cooling occurs in channels that are fed by a converging diverging nozzle.

Our treatment will be:

- one-dimensional (properties uniform across cross-sectional area)
- constant area
- inviscid (no friction)
- heating and/or cooling (no longer adiabatic)

Thus, while the last chapter examined the effect of friction without heat transfer, this chapter considers heat transfer without friction.

There are a number of applications of flow with heat transfer, also called "Rayleigh Flow". Heat exchangers are an obvious example and are found in a wide variety of devices (power cycles, refrigeration, etc.). Flows with combustion and evaporation/condensation can also be modeled using the analysis developed in this chapter. Combustion, evaporation, and condensation in an adiabatic channel are not actually flows with heat transfer to the environment, but rather chemical (in the case of combustion) or phase-change (evaporation and condensation) phenomena that result in the release or absorption of "latent" heat in the flow. These processes can be modeled as heat transfer processes, although the analysis presented here assumes calorically perfect gas and cannot treat the thermochemical changes in the gas as a result of combustion, for example. Nonetheless, combustion of a fuel in air (which is 80% inert nitrogen) results in only a comparatively small change in the thermochemical properties of the combustion products as compared to the initial air, permitting combustion processes to be modeled as the addition of heat from an external source to a mechanical working "fluid" (i.e., air). Indeed, the fact that combustion can release large quantities of heat quickly in a flow (as compared to the effect of wall friction) makes it a particularly good problem for the application of the analysis we will develop here. Thus, a number of our example problems will be drawn from flows with combustion.

Other types of heat transfer interactions include heating via electromagnetic interaction (RF heating, electrical discharge, etc.), lasers, etc.

## 11.1 Effect of Heat Transfer

As with isentropic flow and frictional flow, we will begin by examining differential relations to see how flow responds to heat transfer. The governing equations for constant area flow with heat transfer are:

| | Control Volume | Differential |
|---|---|---|
| Continuity | $\rho_1 \boldsymbol{V}_1 = \rho_2 \boldsymbol{V}_2$ | $\frac{d\rho}{\rho} + \frac{dV}{V} = 0$ |
| Momentum | $p_1 + \rho_1 V_1^2 = p_2 + \rho_2 V_2^2$ | $dp + \rho V dV = 0$ |
| Energy | $\Delta q_{1\text{-}2} = \left(h_2 + \frac{V_2^2}{2}\right) - \left(h_1 + \frac{V_1^2}{2}\right) = h_{o2} - h_{o1}$ | $dh + VdV = dh_o = dq$ |

Note that the momentum equation has no force term: in a constant area channel without friction, there is no way for the channel to exert a force on the flow in the $x$-direction. Note that the energy equation must include a term for the heat transfer $\delta q$ [J/kg]. For a calorically perfect gas, $h = c_p T$, so the different energy equation can be written:

$$c_p dT + VdV = dq \tag{11.1a}$$

$$c_p dT_o = dq \tag{11.1b}$$

From (11.1b), we can see that *positive heat transfer* ($dq > 0$) goes directly into *increasing stagnation temperature* $T_o$. Thus, $T_o$ is no longer constant in flow with heat transfer, and we must exercise caution in using stagnation temperature as a reference state.

We would next like to see how velocity responds to heat transfer by finding a relation analogous to $\frac{dV}{V} = \frac{1}{(M^2-1)}\frac{dA}{A}$ for isentropic flow. Starting with the differential energy equation (11.1a):

$$c_p dT + V dV = dq$$

We can divide through by $dV$:

$$\frac{dq}{dV} = c_p \frac{dT}{dV} + V \tag{11.2}$$

The left hand side is what we are interested in: how an increment of heat transfer $dq$ results in an change in velocity $dV$. The right hand side, however, has another differential $dT$, and we do not know how $dT$ responds to $dq$. Thus, we need to invoke more differentials so that we can isolate just the effect of $dq$ on $dV$. By starting with the equation of state, $p = \rho RT$, we can use logarithmic differentiation to obtain:

$$\frac{dp}{p} = \frac{d\rho}{\rho} + \frac{dT}{T} \tag{11.3}$$

By using continuity $\left(\frac{d\rho}{\rho} = -\frac{dV}{V}\right)$ and writing $\frac{dp}{p}$ as $\frac{dp}{\rho}\frac{1}{RT}$ combined with momentum $\left(\frac{dp}{\rho} = -VdV\right)$, we can re-write (11.3) as:

$$\frac{-VdV}{RT} = -\frac{dV}{V} + \frac{dT}{T}$$

$$\frac{dT}{dV} = \frac{T}{V} - \frac{V}{R} \tag{11.4}$$

Substituting (11.4) into (11.2), we can eliminate all of the differentials except for $dq$ and $dV$.

$$\frac{dq}{dV} = c_p\left(\frac{T}{V} - \frac{V}{R}\right) + V$$

or

$$\frac{dq}{dV} = c_p\left(\frac{T}{V}\right) - \left(\frac{c_p}{R} - 1\right)V$$

$$\frac{dq}{dV} = c_p\left(\frac{T}{V}\right) - \left(\frac{1}{\gamma - 1}\right)V \tag{11.5}$$

This relation is what we were after: it relates the change in velocity $dV$ to the incremental heat transfer $dq$. Unlike the analogous relations for area change and friction, the right hand side is not exclusively a function of Mach number. However, we can obtain an idea of how velocity responds to heat transfer by examining the low velocity and high velocity limits.

At *low velocity* ($V$ small), the first term on the right hand side of (11.5) will dominate:

$$\frac{dq}{dV} \approx c_p\left(\frac{T}{V}\right)$$

Since $T$ and $V$ are positive (flow assumed to the right), $dV$ and $dq$ are related by:

$$dV \sim dq$$

Thus, positive heat transfer ($dq > 0$) results in an increase in velocity ($dV > 0$).

At *high velocity* ($V$ large), the second term in (11.5) dominates, so that:

$$\frac{dq}{dV} \approx -\left(\frac{1}{\gamma - 1}\right)V$$

So, $dV$ and $dq$ have opposite signs:

$$dV \sim -dq$$

Thus, a positive heat transfer to the fluid results in a decrease in velocity.

At low velocity, heat addition accelerates a fluid, and at high velocity, heat addition decelerates a fluid. There must exist some critical velocity that heat addition is continuously driving the flow toward. This critical case will occur when $\frac{dq}{dV} = 0$. This occurs when:

$$c_p\left(\frac{T}{V}\right) = \left(\frac{1}{\gamma - 1}\right)V$$

Solving for $V$:

$$V_{critical} = \sqrt{\gamma RT} = c \Rightarrow M_{critical} = 1$$

In other words, the critical velocity is when the flow is sonic ($M = 1$). Now we can quantify what we mean by "low velocity" and "high velocity." When the flow is below the critical velocity (i.e., subsonic), heat addition has the effect of accelerating the flow. When it is above the critical velocity (i.e., supersonic), heat addition has the effect of decelerating the flow. In this capacity, positive heat transfer is qualitatively similar to converging area and friction flow: it tends to drive a flow toward sonic.

Negative heat transfer ($dq < 0$, i.e., cooling) has the opposite effect: it decelerates subsonic flow and accelerates supersonic flow. Negative heat transfer is qualitatively similar to a diverging area in isentropic flow.

Note that it is theoretically possible for a flow to continuously accelerate from subsonic to sonic (via heating) and then continue to accelerate to supersonic Mach numbers (via cooling), all in a constant area channel with no physical throat. As intriguing as this possibility sounds, no device has ever been built to demonstrate this possibility. It turns out to be a formidable challenge to extract heat from a supersonic flow in practice, making this possibility difficult to realize experimentally.*

How does static temperature respond to heat transfer? Intuitively, of course, we expect positive heat transfer to increase static temperature. Here, again, we will find compressible fluid flow has more surprises for us. Returning to Eq. 11.4:

$$\frac{dT}{dV} = \frac{T}{V} - \frac{V}{R} \tag{11.4}$$

We can again consider the limits of low velocity and high velocity. At low velocity, $dT \sim dV$, so an accelerating flow increases in temperature. At high velocity, $dT \sim -dV$, so an accelerating flow decreases in temperature. Thus, it appears that, for a given flow, the maximum temperature occurs at the critical velocity between the "low velocity" and "high velocity" regime. What is this critical velocity? We might be tempted to conclude that it is the sonic velocity again (since, so far, that has ended up being the interesting velocity in isentropic and Fanno flow). But, if we examine when $\frac{dT}{dV} = 0$ in (11.4), we see that this maximum temperature occurs as:

$$\frac{T}{V} = \frac{V}{R}$$

$$V_{max\ T} = \sqrt{RT} = \frac{1}{\sqrt{\gamma}}\sqrt{\gamma RT} \Rightarrow M_{max\ T} = \frac{1}{\sqrt{\gamma}}$$

Thus, the maximum temperature occurs at Mach number $M = \frac{1}{\sqrt{\gamma}}$, which for $\gamma = 1.4$ is $M = 0.845$. Below this Mach number, positive heat transfer to the flow accelerates the flow and increases static temperature. Between $M = 0.845$ and Mach 1, a very unusual phenomenon occurs: positive heat transfer

*There is a natural phenomenon called "pathological detonation" in which exothermic chemical reactions ($dq > 0$) followed by endothermic reactions ($dq < 0$) permit a flow to pass smoothly from subsonic to supersonic flow in the constant-area reaction zone of a detonation wave.

accelerates the flow while static temperature *decreases*. It may seem unbelievable that we can *pump heat into a gas* and measure a temperature *decrease*, but what is happening is that the heat we are adding is going more toward accelerating the flow than it is increasing its temperature. At supersonic Mach numbers, heat transfer decelerates the flow and increases static temperature, consistent with our intuition. To summarize:

- $M < \frac{1}{\sqrt{\gamma}} \quad \Rightarrow$ heat transfer accelerates flow, increases $T$
- $\frac{1}{\sqrt{\gamma}} < M < 1 \Rightarrow$ heat transfer accelerates flow, decreases $T$
- $M > 1 \quad \Rightarrow$ heat transfer decelerates flow, increases $T$

Finally, it is worth pointing out that the momentum equation $dp + \rho V dV = 0$ still dictates that an increase in velocity must result in a decrease in pressure, and vice versa.

Now we know how the flow properties of interest ($T_o$, $V$, $T$, $p$) respond to heat transfer. We can now develop integral relations that relate conditions at one point in a channel flow to another.

## 11.2 Working Relations for Heat Transfer Flow

For flow that undergoes a finite change in properties as it flows from station 1 to station 2 in a constant area flow, we have already seen from the energy equation that the heat addition (or removal) goes directly to increasing (or decreasing) the stagnation temperature:

$$\delta q = \left(h_2 + \frac{V_2^2}{2}\right) - \left(h_1 + \frac{V_1^2}{2}\right) = h_{o2} - h_{o1}$$

$$\delta q = c_p(T_{o2} - T_{o1})$$

$$T_{o2} - T_{o1} = \frac{\delta q}{c_p} \tag{11.6}$$

The momentum equation

$$p_1 + \rho_1 V_1^2 = p_2 + \rho_2 V_2^2$$

permits us to determine the ratio of static pressures. Using $\rho V^2 = \gamma p M^2$:

$$p_1(1 + \gamma M_1^2) = p_2(1 + \gamma M_2^2)$$

$$\frac{p_2}{p_1} = \frac{1 + \gamma M_1^2}{1 + \gamma M_2^2} \tag{11.7}$$

The stagnation pressure at each point in the flow is related to static pressure by:

$$\frac{p_o}{p} = \left[1 + \frac{\gamma - 1}{2} M^2\right]^{\frac{\gamma}{\gamma - 1}}$$

Note that this relation is valid for each point in the flow, even though (as we will see) $p_o$ is not constant throughout the flow. Thus, we can find the ratio $\frac{p_{o2}}{p_{o1}}$:

$$\frac{p_{o2}}{p_{o1}} = \frac{p_2\left(\frac{p_{o2}}{p_2}\right)}{p_1\left(\frac{p_{o1}}{p_1}\right)} = \left(\frac{1 + \gamma M_1^2}{1 + \gamma M_2^2}\right)\left(\frac{1 + \frac{\gamma - 1}{2} M_2^2}{1 + \frac{\gamma - 1}{2} M_1^2}\right)^{\frac{\gamma}{\gamma - 1}} \tag{11.8}$$

From the relation for pressure $\frac{p_2}{p_1}$, we can find the ratio of static temperature by using the equation of state:

$$\frac{T_2}{T_1} = \frac{p_2}{p_1}\frac{\rho_1}{\rho_2}$$

and the continuity equation $\frac{\rho_1}{\rho_2} = \frac{V_2}{V_1}$:

$$\frac{T_2}{T_1} = \frac{p_2 V_2}{p_1 V_1} = \frac{p_2 M_2 c_2}{p_1 M_1 c_1} = \frac{p_2 M_2}{p_1 M_1}\sqrt{\frac{T_2}{T_1}} \Rightarrow \frac{T_2}{T_1} = \left(\frac{p_2 M_2}{p_1 M_1}\right)^2$$

$$\frac{T_2}{T_1} = \left(\frac{1+\gamma M_1^2}{1+\gamma M_2^2}\right)^2 \left(\frac{M_2}{M_1}\right)^2 \tag{11.9}$$

The stagnation temperature ratio can be expressed as:

$$\frac{T_{o2}}{T_{o1}} = \frac{T_2\left(\frac{T_{o2}}{T_2}\right)}{T_1\left(\frac{T_{o1}}{T_1}\right)}$$

$$\frac{T_{o2}}{T_{o1}} = \left(\frac{M_2}{M_1}\right)^2 \left(\frac{1+\gamma M_1^2}{1+\gamma M_2^2}\right)^2 \left(\frac{1+\frac{\gamma-1}{2}M_2^2}{1+\frac{\gamma-1}{2}M_1^2}\right) \tag{11.10}$$

Similarly, we can find expressions for $\frac{\rho_2}{\rho_1}$, etc.

Note that Eq. 11.10, which was derived from the momentum equation, gives the ratio of stagnation temperatures, but Eq. 11.6 (the energy equation) also relates the change in stagnation temperature to the heat addition.*

$$T_{o2} - T_{o1} = \frac{\delta q}{c_p} \tag{11.6}$$

*The flow we are studying in this chapter, Rayleigh Flow, when applied to a calorically perfect gas, is sometimes referred to as "Simple $T_o$-Change Flow."

Thus, given an initial Mach number $M_1$ and the stagnation temperature $T_{o1}$, if we know the amount of heat addition $\delta q$ to the flow as it travels through a length of constant area channel, we can find the new stagnation temperature $T_{o2}$ and, using Eq. 11.10, the new Mach number $M_2$. Once the Mach number is known, the relations for static pressure (11.7), stagnation pressure (11.8), and temperature (11.9) permit us to find the rest of the properties at the new location.

Unfortunately, Eq. 11.10 (similar to the relations for area ratio in isentropic flow and channel length in frictional flow) cannot be directly solved for $M_2$ given $M_1$. Thus, it becomes convenient to define a reference state and tabulate values of these ratios. Since heat addition always drives a flow to Mach 1, the sonic conditions become a convenient reference state, which we will denote with ( $^*$ ). Taking our relations and setting $M_1 = M$ and $M_2 = 1$, we obtain:

$$\frac{T}{T^*} = \left(\frac{1+\gamma}{1+\gamma M^2}\right)^2 M^2 \tag{11.11}$$

$$\frac{p}{p^*} = \frac{1+\gamma}{1+\gamma M^2} \tag{11.12}$$

$$\frac{T_o}{T_o^*} = \frac{2(\gamma+1)M^2\left(1+\frac{\gamma-1}{2}M^2\right)}{(1+\gamma M^2)^2} \tag{11.13}$$

$$\frac{p_o}{p_o^*} = \frac{\gamma+1}{1+\gamma M^2}\left[\frac{2\left(1+\frac{\gamma-1}{2}M^2\right)}{\gamma+1}\right]^{\frac{\gamma}{\gamma-1}} \tag{11.14}$$

These values are tabulated as a function of Mach number in Table A-5.

The use of these relations are best illustrated via a numerical example.

## 11.2.1 Numerical Example: Heat Addition to a Supersonic Flow

**Problem:** Air enters a channel at Mach 0.7 and with temperature and pressure of 300 K and 1 atm, respectively. The channel is without friction, but there is heat transfer.

(a) Find the amount of heat transfer $\delta q^*$ [kJ/kg] necessary to bring the flow exiting the pipe to sonic conditions. Also find the exit temperature, pressure, and stagnation pressure in this case.

(b) Find the amount of heat transfer $\delta q$ [kJ/kg] if the flow exits the channel at Mach 0.5. Also find the exit temperature, pressure, and stagnation pressure in this case.

**Solution:** We start, as always, by finding the reference states of the flow at the entrance of the channel. For a flow at Mach 0.7, isentropic relations give us the stagnation conditions:

$$M_1 = 0.7 \Rightarrow \frac{T}{T_o} = 0.91075 \Rightarrow T_{o1} = 329.4 \text{ K}$$

$$M_1 = 0.7 \Rightarrow \frac{p}{p_o} = 0.72092 \Rightarrow p_{o1} = 1.3871 \text{ atm}$$

(a) Heat Transfer brings Flow to Sonic

Since we know the inlet Mach number and the fact that the flow exits the channel as sonic, then the change in To is given by (from either Eq. 11.13 or Table A-5):

$$M_1 = 0.7 \Rightarrow \frac{T_{o1}}{T_o^*} = 0.90850 \Rightarrow T_o^* = 362.6 \text{ K}$$

Knowing the new value of $T_o$, the heat transfer is given by the energy equation (Eq. 11.6):

$$\delta q^* = c_p(T_o^* - T_{o1}) = \left(1.0035 \frac{\text{kJ}}{\text{kg K}}\right)(362.6 \text{ K} - 329.4 \text{ K}) = 33.3 \frac{\text{kJ}}{\text{kg}}$$

Thus, $\delta q^* = 33.3$ kJ/kg. The sonic temperature, pressure, and stagnation pressure come directly from Eqs. 11.12-14:

$$M_1 = 0.7 \Rightarrow \frac{p_1}{p^*} = 1.4235 \Rightarrow p^* = 0.702 \text{ atm}$$

$$M_1 = 0.7 \Rightarrow \frac{T_1}{T^*} = 0.99289 \Rightarrow T^* = 302 \text{ K}$$

$$M_1 = 0.7 \Rightarrow \frac{p_{o1}}{p_o^*} = 1.0431 \Rightarrow p_o^* = 1.330 \text{ atm}$$

Thus, we see the positive heat addition is required to accelerate the flow to sonic, resulting in a decrease in the static pressure. The stagnation pressure also decreases due to heat addition. Static temperature at the exit ($T^* = 302$ K) is nearly identical to the inlet ($T_1 = 300$ K). This result may seem unusual, but recall in the range $0.845 < M < 1$ that static temperature actually decreases with heat addition, so the static temperature increased then decreased as Mach number passed from 0.7 to 1.0.

(b) Heat Transfer brings Flow to Mach 0.5

Since we know the exit Mach number ($M_2 = 0.5$), we can find the ratio of stagnation temperatures from Eq. 11.10. If we wish to use the tabulated data in Table A-5, we can do so, since we know the sonic conditions from our solution of part (a):

$$M_2 = 0.5 \Rightarrow \frac{T_{o2}}{T_o^*} = 0.69136 \Rightarrow T_{o2} = 250.7 \text{ K}$$

Note that the sonic conditions ($T_o^*$, etc.) from part (a) still apply in (b), even though the flow does not reach sonic in this part. Knowing $T_{o2}$, we can find $\delta q$:

$$\delta q = c_p(T_{o2} - T_{o1}) = \left(1.0035\frac{\text{kJ}}{\text{kg K}}\right)(250.7\text{ K} - 329.4\text{ K}) = -79.0\frac{\text{kJ}}{\text{kg}}$$

The negative value of heat transfer denotes the fact that heat was transferred *out* of the flow, i.e., cooling. Heat transfer out of a flow has the effect of driving the flow further from sonic, which was the case here.

We can also find temperature, pressure, and stagnation pressure by relating them to the sonic conditions found in part (a).

$$M_2 = 0.5 \Rightarrow \frac{p_2}{p^*} = 1.7778 \Rightarrow p_2 = 1.248\text{ atm}$$

$$M_2 = 0.5 \Rightarrow \frac{T_2}{T^*} = 0.79012 \Rightarrow T_2 = 238.6\text{ K}$$

$$M_2 = 0.5 \Rightarrow \frac{p_{o2}}{p_o^*} = 1.1140 \Rightarrow p_{o2} = 1.4816\text{ atm}$$

Note that the static pressure is higher at the exit because the flow has slowed down. Static temperature decreased due to cooling. Interesting, stagnation pressure increases; this may seem to contradict what has been discussed earlier regarding the fact that stagnation pressure must always decrease, reflecting an increase in entropy. Here, however, heat was transferred out of the system to the surrounding environment, permitting entropy for the system to decrease.

## 11.3 Effect of Increasing Heat Addition*

Heat addition, like area convergence and friction, can choke a flow. Once the amount of heat has been added to bring the flow to sonic conditions in a constant area channel (max heat: $\delta q^*$), no more heat may be added without modifying the flow conditions at the entrance to the channel.

In a *subsonic* channel flow, if the amount of heat addition exceeds $\delta q^*$ as defined by the inlet conditions, the inlet Mach number and mass flow rate will decrease so that the new amount of heat addition will bring the flow to sonic. Since increasing the heat addition necessitates a decrease in mass flow, we can say the flow is *thermally choked*. This is similar to how a converging area in isentropic flow and increasing channel length in frictional flow modify the upstream subsonic flow to maintain choked conditions.

In a *supersonic* flow, increasing heat addition beyond the value necessary to bring the flow to sonic will result in a normal shock wave forming upstream. The normal shock appears upstream of the heat addition section (in the nozzle, if the channel is being fed supersonic flow from a converging-diverging nozzle). Note that the shock does *not* appear in the channel (as was the case in Fanno flow), because a shock wave is adiabatic and does not change the value of $T_o$. Thus, if the heat addition $\delta q^*$ is sufficient to increase the original $T_o$ to $T_o{}^*$, it will do so regardless of whether the flow is supersonic or subsonic flow emerging from a normal shock at the same supersonic Mach number. Only by forcing the shock into the diverging nozzle will the Mach number at the channel inlet decrease to enable the flow to be able to accept more heat and still reach sonic conditions at the end. As the heat addition is increased further, the shock is forced further upstream, until it will eventually reach the throat. At this point, further increases in heat addition will result in subsonic flow throughout and mass flow rate through the channel will decrease. These scenarios are illustrated below.

*The effect of heat addition is discussed in greater detail in a classic paper: J.V. Foa and G. Rudinger, "On the Addition of Heat to a Gas Flowing in a Pipe at Subsonic Speed," *Journal of the Institute of Aeronautical Sciences*, Vol. 16, No. 2, Feb. 1949.

Effect of Increasing Heat Addition
to Choked Subsonic Flow

thermally choked

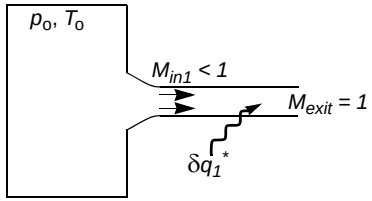


increasing heat addition: $\delta q_2^* > \delta q_1^*$

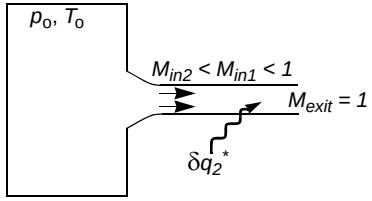


$\Rightarrow M_{in}$ decreases
$\Rightarrow$ mass flow decreases
$\Rightarrow$ exit conditions still sonic

Effect of Increasing Heat Addition
to Choked Supersonic Flow

thermally choked

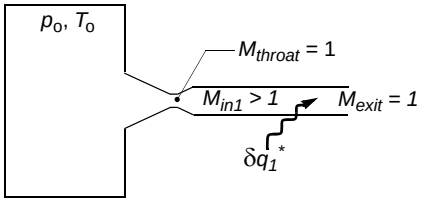


increasing heat addition: $\delta q_2^* > \delta q_1^*$

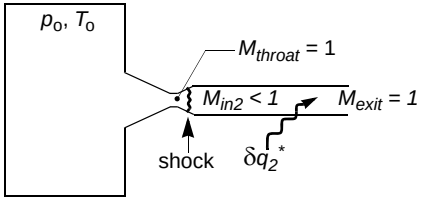


$\Rightarrow$ shock forms in nozzle
$\Rightarrow$ mass flow constant
$\Rightarrow$ exit conditions still sonic

increasing heat addition further: $\delta q_3^* > \delta q_2^*$

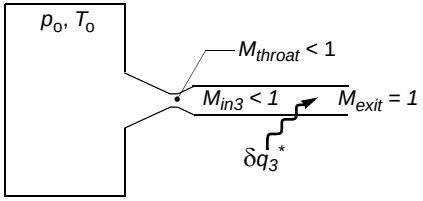


$\Rightarrow$ shock forced to throat
$\Rightarrow$ mass flow decreases with further increase in $\delta q$
$\Rightarrow$ exit conditions still sonic

# 12. Oblique Shock Waves

This chapter begins our discussion of two-dimensional, steady supersonic flow. In this chapter, we will examine shock waves that result when supersonic flow encounters a *compressive corner* (i.e., a corner that turns *into* the flow). The abrupt change in flow direction results in a shock wave, but the shock wave can now be at an angle with respect to the flow rather than normal; such a shock wave is termed an *oblique shock*. In the next chapter, we will examine the flow over an *expansive corner* (i.e., a corner that turns *away* from the flow).

Oblique shock waves are encountered in external supersonic flow (the flow over wings and fuselages) and in internal flows where the area change is not gradual (i.e., supersonic inlet/diffusers). Oblique shocks also appear when converging/diverging nozzles exhaust into a chamber in which the back pressure does not exactly match the exit pressure (overexpanded and underexpanded nozzles). These applications are treated in Chapter 14.

## 12.1 Oblique Shocks Derived from Normal Shocks

To begin our study of oblique shock waves, we will return to the normal shock wave of Chapter 7. Consider a steady shock wave:

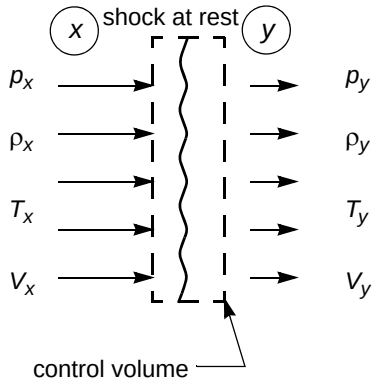


Recall that we can make any shock wave steady by transforming into its reference frame. Now, consider if we transform into a reference frame moving perpendicular to the normal shock (i.e., moving up or down along the shock). We can do this by adding a velocity $V_T$ (tangential) to the picture above:

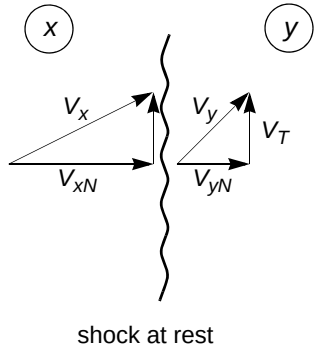


shock at rest

We will denote the original velocities normal to the wave as $V_{xN}$ and $V_{yN}$, and the resultant velocities as $V_x$ and $V_y$. If we simply rotate the above picture in the clockwise direction, we obtain:

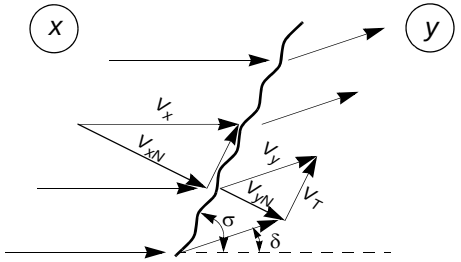


We can interpret this picture as a steady, supersonic flow approaching from the left at velocity $V_x$, and then being deflected upward at an angle $\delta$, the *deflection angle* or *wedge angle*. The angle between the resulting shock and the incoming flow is $\sigma$, the *shock angle*.*

*Suggested mnemonic devise: "***s**igma" for ***s**hock, "***d**elta" for ***d**eflection.

The goal is to now develop a set of relations for oblique shock waves that are analogous to the normal shock relations developed in Section 7. Our shock relations will now have to include the geometric parameters $\sigma$ and $\delta$.

## 12.2 Oblique Shock Relations

We begin with an oblique shock and draw a control volume around the wave:

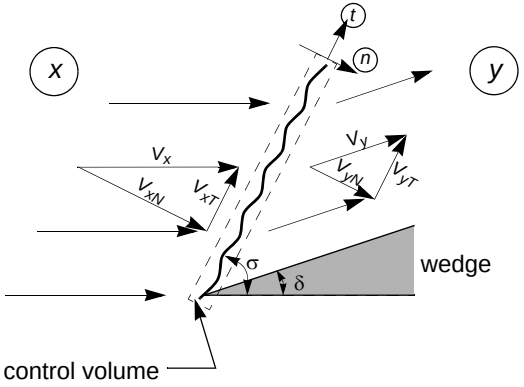


We still use *x* and *y* to denote conditions upstream and downstream of the shock, and the velocities are decomposed into components normal and tangential to the oblique shock. Applying the continuity relations to this steady wave:

$$\int_{CS} \rho \vec{V} \cdot d\vec{A} = 0$$

$$\rho_x V_{xN} = \rho_y V_{yN}$$

Note that we can always shrink the control volume so close to the shock that the upstream and downstream area will be equal, and there will be negligible mass flow through the sides of the control volume. Thus, density and the normal component of velocity are related by:

$$\frac{\rho_y}{\rho_x} = \frac{V_{xN}}{V_{yN}} \tag{12.1}$$

Next, to apply the steady momentum equation:

$$\Sigma \vec{F} = -\int_{CS} \vec{V}(\rho \vec{V} \cdot d\vec{A})$$

Recall that the momentum equation is a *vector* equation, with components in both the normal and tangential directions:

Normal Direction: $$(p_y - p_x)A = \dot{m}(V_{xN} - V_{yN}) \tag{12.2}$$

Tangential Direction: $$0 = \dot{m}(V_{xT} - V_{yT}) \tag{12.3}$$

Again, we will neglect the mass flow through the sides of the control volume by taking it as very thin. Note that the tangential component of the momentum equation tells us that:

$$V_{xT} = V_{yT} \tag{12.4}$$

In other words, we must add the same tangential velocity to both sides of the normal shock to transform to an oblique shock; we had already done this in Section 12.1. Another way to interpret this result is that there can be no change in tangential velocity as we cross an oblique shock; the shock only affects the normal component of velocity.

Finally, we apply the energy equation for a steady, adiabatic control volume:

$$\int_{CS} \left(h + \frac{V^2}{2}\right) \rho \vec{V} \cdot d\vec{A} = 0$$

which reduces to:

$$h_{ox} = h_x + \frac{V_x^2}{2} = h_y + \frac{V_y^2}{2} = h_{oy} \tag{12.5}$$

Recall that energy is a *scalar*, it deals with the magnitude of the resultant velocity, not the components. If we want to express the energy equation in terms of the velocity components, we can use:

$$V_x^2 = V_{xT}^2 + V_{xN}^2$$

$$V_y^2 = V_{yT}^2 + V_{yN}^2$$

Substituting into the energy equation:

$$h_x + \frac{V_{xT}^2 + V_{xN}^2}{2} = h_y + \frac{V_{yT}^2 + V_{yN}^2}{2}$$

Since we know from momentum that $V_{xT} = V_{yT}$, the tangential components of velocity cancel out:

$$h_x + \frac{V_{xN}^2}{2} = h_y + \frac{V_{yN}^2}{2} \neq h_o \tag{12.7}$$

However, this resulting expression is *not* the total enthalpy of the flow.

Our goal is now to manipulate these expressions of the conservation laws into a form that gives us $\frac{p_y}{p_x}$, $\frac{T_y}{T_x}$, etc. as functions of upstream Mach number $M_x$ and the shock angle $\sigma$.

From momentum:

$$\frac{p_y}{p_x} - 1 = \frac{\dot{m}}{p_x A}\left(V_{xN} - \frac{V_{yN}}{V_{xN}} V_{xN}\right)$$

Using continuity ($\frac{\rho_y}{\rho_x} = \frac{V_{xN}}{V_{yN}}$):

$$\frac{p_y}{p_x} - 1 = \frac{\rho_x V_{xN}^2 A}{p_x A}\left(1 - \frac{\rho_x}{\rho_y}\right)$$

which simplifies to:

$$\frac{p_y}{p_x} = 1 + \gamma M_x^2 \sin^2\sigma\left(1 - \frac{\rho_x}{\rho_y}\right) \tag{12.8}$$

This is an expression for $\frac{p_y}{p_x}$, but it is in terms of $\frac{\rho_x}{\rho_y}$. To find another relation, we turn to the energy equation:

$$h_x + \frac{V_{xN}^2}{2} = h_y + \frac{V_{yN}^2}{2}$$

Using calorically perfect gas assumption:

$$c_p T_x + \frac{V_{xN}^2}{2} = c_p T_y + \frac{V_{yN}^2}{2}$$

Using $c_p = \frac{\gamma}{\gamma - 1} R$, $T = \frac{p}{\rho R}$, and, from continuity, $V_{yN} = \frac{\rho_x}{\rho_y} V_{xN}$:

$$\frac{\gamma}{\gamma - 1} R \frac{p_x}{\rho_x R} + \frac{V_{xN}^2}{2} = \frac{\gamma}{\gamma - 1} R \frac{p_y}{\rho_y R} + \left(\frac{\rho_x}{\rho_y}\right)^2 \frac{V_{xN}^2}{2}$$

Which can be simplified to:

$$\frac{\gamma}{\gamma - 1}\left(\frac{p_y}{\rho_y} - \frac{p_x}{\rho_x}\right) = \frac{V_{xN}^2}{2}\left[1 - \left(\frac{\rho_x}{\rho_y}\right)^2\right]$$

Introducing Mach number ($V^2 = \gamma RTM^2$) and $\sigma$ ($V_{xN} = V_x \sin\sigma$):

$$\frac{p_y}{p_x} = \frac{\rho_y}{\rho_x}\left[\frac{\gamma-1}{2}M_x^2\sin^2\sigma\left(1-\left(\frac{\rho_y}{\rho_x}\right)^2\right)+1\right] \tag{12.8}$$

This gives us another expression for $\frac{p_y}{p_x}$ also in terms of $\frac{\rho_y}{\rho_x}$. Since (12.7) and (12.8) must both hold, we can solve for $\frac{p_y}{p_x}$ and $\frac{\rho_y}{\rho_x}$:

$$\boxed{\frac{p_y}{p_x} = \frac{2\gamma M_x^2\sin^2\sigma-(\gamma-1)}{\gamma+1}} \tag{12.9}$$

$$\boxed{\frac{\rho_y}{\rho_x} = \frac{(\gamma+1)M_x^2\sin^2\sigma}{2+(\gamma-1)M_x^2\sin^2\sigma}} \tag{12.10}$$

And temperature is given by:

$$\boxed{\frac{T_y}{T_x} = \frac{p_y\rho_x}{p_x\rho_y} = \left[\frac{2\gamma M_x^2\sin^2\sigma-(\gamma-1)}{\gamma+1}\right]\left[\frac{2+(\gamma-1)M_x^2\sin^2\sigma}{(\gamma+1)M_x^2\sin^2\sigma}\right]} \tag{12.11}$$

Thus, we have our working relations for pressure, density, and temperature. This exercise, however, was largely unnecessary. If we examined the conservation laws for the oblique shock (12.1-12.7), they are identical to the conservation laws for a normal shock wave, where we use $V_{xN}$ instead of $V_x$ in the normal shock relations. Thus, all of our normal shock relations developed in Chapter 7 are still valid, and indeed are identical to (12.9-12.11), *provided we use the normal component of velocity and Mach number.* Recall from the earlier part of this chapter (Section 12.1), an oblique shock can be "constructed" from a simple coordinate transformation of a normal shock. Thus, it should not be surprising that our normal shock relations are valid, provided we use only the normal components of velocity.

From the geometry of the oblique shock:

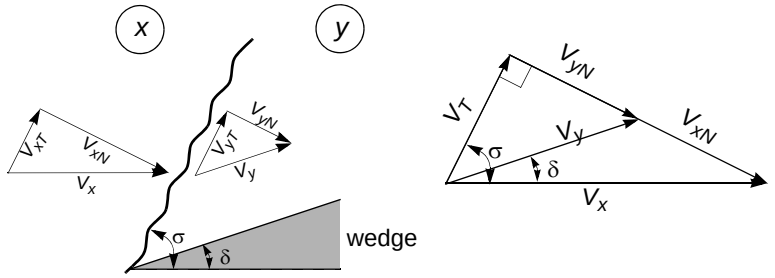


the normal components of velocity and Mach number are:

$$V_{xN} = V_x\sin\sigma$$

$$M_{xN} = M_x\sin\sigma \tag{12.12}$$

Therefore, knowing $M_x$ and $\sigma$, we can use the normal shock relations or the tabulated values given in table A-3, provided we use $M_{xN}$ in place of $M_x$. The normal shock relations (or tables) will give or $\frac{p_y}{p_x}$, $\frac{\rho_y}{\rho_x}$, and $\frac{T_y}{T_x}$. They also give the value of $M_{yN}$, the normal component of Mach number downstream of the oblique shock. To relate this to the resultant downstream Mach number, we again refer to the geometry of the oblique shock:

$$V_{yN} = V_y\sin(\sigma-\delta)$$

Normalizing by $c_y$:

$$\boxed{M_y = \frac{M_{yN}}{\sin(\sigma-\delta)}} \tag{12.13}$$

Note that we require the deflection angle (wedge angle) $\delta$ in order to convert $M_{yN}$ to $M_y$. From the geometry of the oblique shock:

$$V_{yN} = V_{yT}\tan(\sigma - \delta)$$

$$V_{xN} = V_{xT}\tan(\sigma)$$

Thus, from geometry:

$$\frac{V_{yN}}{V_{xN}} = \frac{\tan(\sigma - \delta)}{\tan(\sigma)}$$

But the continuity equation shows that $\frac{V_{yN}}{V_{xN}} = \frac{\rho_x}{\rho_y}$, and we already have an expression for $\frac{\rho_y}{\rho_x}$ in terms of $M_x$ and $\sigma$. Thus, equating these:

$$\frac{\tan(\sigma - \delta)}{\tan(\sigma)} = \frac{V_{yN}}{V_{xN}} = \left(\frac{\rho_y}{\rho_x}\right)^{-1} = \left(\frac{(\gamma+1)M_x^2\sin^2\sigma}{2 + (\gamma-1)M_x^2\sin^2\sigma}\right)^{-1}$$

Thus, $\sigma$, $\delta$, and $M_x$ are related by the above expression. Solving for $\delta$:

$$\boxed{\tan\delta = \frac{(M_x^2\sin^2\sigma - 1)\cot\sigma}{\frac{\gamma+1}{2}M_x^2 - M_x^2\sin^2\sigma + 1}} \qquad (12.14)$$

This relation* links $\sigma$, $\delta$, and $M_x$.

*Recall $\cot\theta = \frac{1}{\tan\theta}$.

These relations are sufficient to solve any oblique shock problem. Given any *two* of these parameters: $M_x$, $M_y$, $\sigma$, $\delta$, and $\frac{p_y}{p_x}$ (or $\frac{\rho_y}{\rho_x}$ or $\frac{T_y}{T_x}$), you can solve for the rest using Eqs. 12.9-12.14. Before applying these relations, however, some discussion on how these variables are related is in order.

The shock angle $\sigma$ cannot assume any arbitrary value. As shown in Chapter 7, a normal shock wave must be supersonic. For an oblique shock, this means that the normal component of velocity into the shock must be supersonic:

$$M_{xN} \geq 1$$

Or:

$$M_x\sin\sigma \geq 1$$

$$\sigma \geq \sin^{-1}\frac{1}{M}$$

Thus, the shock angle $\sigma$ must be at least equal to or greater than the Mach angle $\alpha$. This makes sense: the Mach angle is the wave angle caused by a point-disturbance. The shock wave generated by a wedge will be a stronger disturbance than this, so it will be more inclined to the flow. The shock caused by a very small deflection angle (i.e., a wedge that approached $\delta = 0°$) approaches a sound wave and should asymptote to the Mach angle. Indeed, it can be shown that for Eq. 12.14, as deflection angle $\delta \to 0$, shock angle $\sigma \to \alpha$.

The maximum value of shock angle $\sigma$ is 90°, corresponding to a normal shock. For a fixed upstream Mach number $M_x$, between $\sigma = \alpha$ and $\sigma = 90°$, there is an entire family of oblique shock solutions, each one corresponding to a unique wedge angle $\delta$. We can plot $\delta$ vs. $\sigma$ for a fixed Mach number (Eq. 12.14); here it has been plotted for $M_x = 3$ and $\gamma = 1.4$. As discussed above, the minimum value of shock angle is $\sigma_{min} = \alpha = \sin^{-1}\frac{1}{M} = 19.47°$, which corresponds to zero deflection angle ($\delta = 0°$). The normal shock case ($\sigma = 90°$) also corresponds to zero deflection angle. Note that in between these two values,

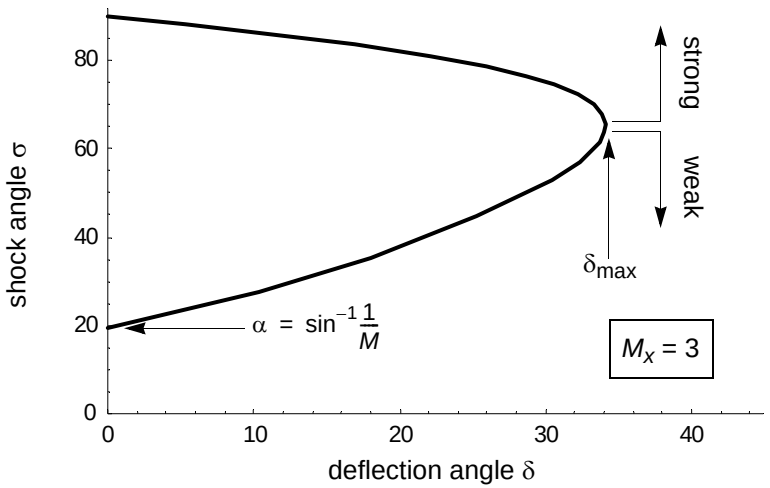


the deflection angle is finite, and reaches a maximum value of $\delta_{max} = 34.1°$ for $M_x = 3$, at which condition $\sigma = 65.2°$. This maximum defines two branches of the oblique shock solution, one with oblique shocks that are more steeply inclined to the flow, called *strong* oblique shocks, and the other with shocks more "laid back" to the flow, called *weak* oblique shocks.

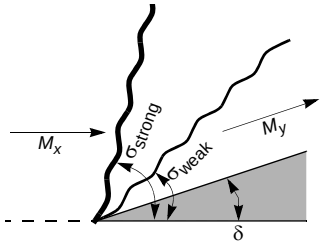


The fact that there exists two branches of the oblique shock solution means that (for a given Mach number $M_x$), if the deflection angle is specified (e.g., a fixed wedge angle), there are *two* possible oblique shock angles $\sigma$ that will give very different values of post-shock properties. The strong shock will give a much larger increase in pressure, temperature, etc., and result in a much more significant deceleration of the flow as compared to the weak shock. For a given experimental situation, however, only one oblique shock is typically observed. For external flows, the *weak oblique shock solution is almost always obtained*. For internal flows, the weak solution is also usually observed, although it is possible to force the strong oblique shock solution by modifying the downstream conditions (back pressure, etc.). The usual convention is to *always use the weak shock solution*, unless specified otherwise.

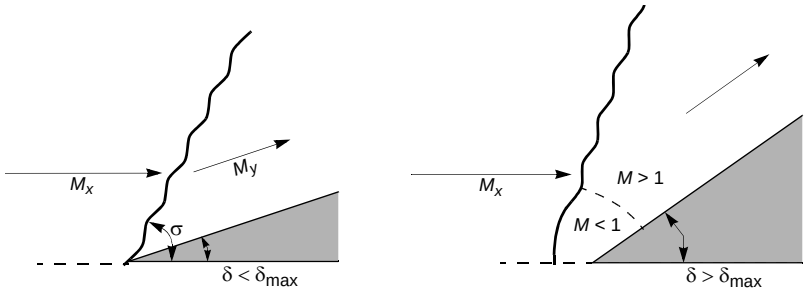


The existence of a maximum deflection angle means that, as the wedge angle is increase beyond this certain maximum $\delta_{max}$, there is no oblique shock solution permitted. In this case, the oblique shock becomes a *detached* bow shock, and moves upstream of the corner and stabilizes in the flow as a normal shock that decays to an oblique shock away from the wall. This case is difficult to analyze; the flow downstream of the shock contains a pocket of subsonic flow which reaccelerates to supersonic flow. Although this case is frequently encountered, it will not be discussed further here.

It is possible to determine the shock angle $\sigma$ when the maximum deflection angle $\delta_{max}$ is encountered:

$$\sin^2\sigma_{\delta max} = \frac{1}{\gamma M_x^2}\left\{\frac{\gamma+1}{4}M_x^2 - 1 + \left[(\gamma+1)\left(1 + \frac{\gamma-1}{2}M_x^2 + \frac{\gamma+1}{16}M_x^4\right)\right]^{\frac{1}{2}}\right\}$$

Note that this is *not* the maximum value of $\sigma$ ($\sigma_{max}$ is 90° for all Mach numbers); rather, this is the value of the oblique shock when it is on the verge of becoming a detached shock because the deflection angle is too large. With the value of $\sigma$ known, Eq. 12.14 can be used to find that critical deflection angle. Both $\delta_{max}$ and the corresponding value of $\sigma$ are plotted here. Note that as Mach number increases, the flow can tolerate an increasing wedge angle without becoming detached. In the limit of very large Mach numbers,

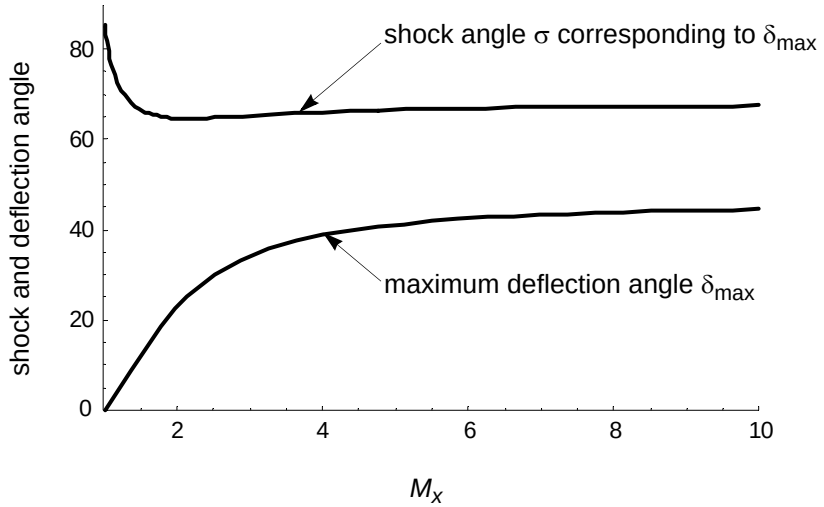


$\delta_{max} \rightarrow 45.37°$ for $\gamma = 1.4$. Thus, an oblique shock can never remain attached to a wedge with deflection angle much greater than 45°.

While the normal component of flow entering an oblique shock must be supersonic, the flow exiting the oblique shock can be subsonic or supersonic. The normal component exiting the wave will, of course, have to be subsonic from our normal shock relations discussed in Chapter 7. But, from Eq. 12.13, the resultant Mach number of the flow leaving the wave can be, and indeed usually is, *supersonic*. Obviously, if the wedge angle is very small and the oblique shock approaches the Mach angle, the flow leaving the wave is almost unchanged from the flow approaching. As the wedge angle (and shock angle) increase, the shock becomes stronger and the flow will be more significantly decelerated, until for a critical shock angle, the exit flow becomes subsonic. This critical shock angle can also be found analytically:

$$\sin^2\sigma_{M_2=1} = \frac{1}{\gamma M_x^2}\left\{\frac{\gamma+1}{4}M_x^2 - \frac{3-\gamma}{4} + \left[(\gamma+1)\left(\frac{9+\gamma}{16} - \frac{3-\gamma}{8}M_x^2 + \frac{\gamma+1}{16}M_x^4\right)\right]^{\frac{1}{2}}\right\}$$

This expression appears similar to the one for maximum deflection angle. Indeed, quantitatively, they turn out to be very close: the condition for maximum deflection occurs near the condition at which the flow exiting the oblique shock becomes subsonic. For the case of Mach 3 flow, $\delta_{sonic} = 34.0°$, $\sigma_{sonic} = 63.8°$.

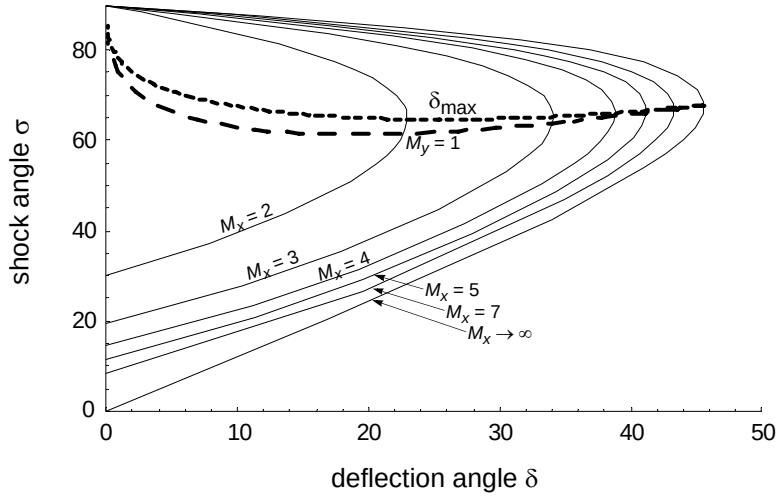


If we generate a family of σ vs. δ curves for different Mach numbers (see above), we can plot the locus of states for maximum deflection angle (dotted line) and sonic exit flow leaving the shock (dashed line). Recall that the maximum deflection angle defines the boundary between strong and weak shock solutions. Thus, the flow exiting a strong oblique shock is always subsonic. For weak oblique shocks, the flow exiting the wave is supersonic, except for a small region of shock angle very near the maximum deflection angle that leads to a detached shock wave. Thus, we can expect most oblique shock problems to exhibit *supersonic flow downstream of the shock.*

This figure (or more elaborate versions of it, such as the "Oblique Shock Chart" given in the Appendix) is very useful for problem solving. Typically in problems, the Mach number and deflection angle is specified and the shock angle σ must be solved for. Eq. 12.14 is cumbersome to invert, so it is convenient to use a graphical presentation of the solution to estimate the value of the shock angle σ for the given $M_x$ and δ. Then, Eq. 12.14 can be used to iterate for the exact value. Once σ is known, the normal component of Mach

number $M_{xN}$ can be used in the normal shock tables to find the properties downstream of the oblique shock.

Oblique shock tables are also available, but these tables tend to be rather bulky, since both $M_x$ and $\delta$ (or $\sigma$) are independent parameters and therefore the tables must be "two-dimensional" rather than our familiar "one-dimensional" normal shock tables. Thus, the chart becomes the preferred solution technique. This procedure is illustrated in the following numerical example:

### 12.2.1 Numerical Example: Oblique Shock Wave in Mach 3 Flow Generated by 10° Wedge

**Problem:** A uniform supersonic flow at Mach 3 and 1 atm static pressure encounters a wedge with deflection angle of 10°. Find the shock angle and the pressure and Mach number downstream of the shock.

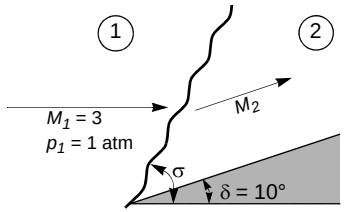


**Solution:** We are asked to find $\sigma$, $M_2$, and $p_2$. Given $M_1$ and $\delta$, we can, in principle, find $\sigma$ from Eq. 12.14, but it is convenient to consult an oblique shock chart (as given in the Appendix). From the chart, it appears that the shock angle for $M_1 = 3$ and $\delta = 10°$ is approximately $\sigma \approx 28°$ (note we assume the weak shock solution). We will use this value as an initial guess and interpolate using Eq. 12.14:

| $\sigma$ | $\delta$ |
|---|---|
| 28° | 10.67° |
| 27° | 9.576° |

Interpolating to obtaining $\delta = 10°$, we find $\sigma = 27.4°$. Knowing $\sigma$, we can compute the normal component of Mach number:

$$M_{xN} = M_x \sin\sigma = 3 \sin 27.4° = 1.38$$

The value of $M_{xN} = 1.38$ can be used directly in the normal shock tables:

$$\left(\frac{p_y}{p_x}\right)_{M_{xN}=1.38} = 2.055$$

$$M_{xN} = 1.38 \Rightarrow M_{yN} = 0.7483$$

Knowing $M_{yN}$ and $\delta$ permits us to find the Mach number of the downstream flow via Eq. 12.13

$$M_y = \frac{M_{yN}}{\sin(\sigma - \delta)} = \frac{0.7483}{\sin(27.4 - 10)} = 2.50$$

Thus, the flow exiting the wave is at $p_2 = 2.055$ atm and at a Mach number $M_2 = 2.50$. Thus, the flow has been decelerated and compressed by the oblique shock, but is still supersonic.

## 12.3 Oblique Shock Reflection

When an oblique shock encounters a wall, it is reflected from the wall back into the flow. The wave reflection is not *spectral*, meaning that, unlike light, the angle of incidence does not equal the angle of reflection. This is because shock waves are *nonlinear waves*: the reflected wave will have a different strength than the incident wave. In general, the reflected wave will be weaker (lower Mach number, lower pressure ratio).

The reflected shock wave, like the original shock wave generated by the wedge, is determined by the flow upstream of the wave and the wall, which determines the direction the flow must follow. Solving for the reflected shock is best illustrated by a numerical example.

## 12.3.1 Numerical Example: Reflection of an Oblique Shock Wave in Mach 3 Flow Generated by 10° Wedge

**Problem:** Returning to the oblique shock in Section 12.2.1, solve for the reflected oblique shock angle and the flow downstream of the reflected shock if there is an upper wall that is parallel to the original flow direction.

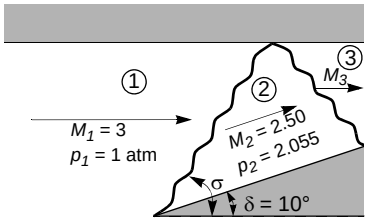


**Solution:** Since the original wedge deflected the flow upward with a deflection angle $\delta_1 = 10°$, the upper wall will deflect the flow back down by the same deflection angle: $\delta_2 = 10°$. If we neglect the incident shock for a moment and just examine the flow downstream, the flow pattern is the same as for the oblique shock problem we have been discussing all along: a supersonic flow encounters a wall inclined to the flow, forcing it to deflect by an amount δ.

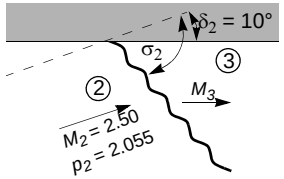


Knowing that the flow is approaching at $M_2 = 2.50$ and the deflection angle is $\delta_2 = 10°$, we can estimate the shock angle $\sigma_2 \approx 32°$ from the oblique shock chart (note that $M_2$ now plays the role of $M_x$). Interpolating Eq. 12.14 to obtain a more exact value for the shock angle:

| σ | δ |
|---|---|
| 32° | 10.15° |
| 31° | 9.092° |

Interpolation yields $\sigma_2 = 31.86°$. With the shock angle known, we can solve for the normal component of flow entering the shock:

$$M_{xN} = M_x \sin\sigma = 2.5 \sin 31.9° = 1.32$$

The value of $M_{xN} = 1.32$ can be used directly in the normal shock tables:

$$\left(\frac{p_y}{p_x}\right)_{M_{xN}=1.32} = 1.866 \Rightarrow p_3 = 3.835 \text{ atm}$$

$$M_{xN} = 1.32 \Rightarrow M_{yN} = 0.776$$

Knowing $M_{yN}$ and δ permits us to find the Mach number of the downstream flow via Eq. 12.13

$$M_y = \frac{M_{yN}}{\sin(\sigma - \delta)} = \frac{0.776}{\sin(31.86 - 10°)} = 2.08$$

Thus, the flow exiting the reflected wave is at $p_3 = 3.825$ atm and at a Mach number $M_3 = 2.08$. Thus, the flow continues to decelerate and the pressure continues to increase. The pressure *ratio* across the second shock, however, is not as great as the first, because the flow was already decelerated by the first shock and therefore the second shock is not as strong.

---

Note that these results match our expectations from isentropic flow: a supersonic flow into a converging area should decelerate while increasing in static pressure. Although a flow with oblique shocks is not isentropic, the stagnation pressure losses across oblique shocks is usually small (this can be verified by examining the values of $\frac{p_{oy}}{p_{ox}}$ for a normal shock of strength $M_{xN}$). Thus, if we compare the results we obtain for flow decelerated by oblique shocks with that obtained via an isentropic diffuser, the results are often in close agreement.

When an oblique shock wave reflects directly from the wall, as in the numerical example of Section 12.3.1, it is termed *regular reflection*. Oblique shocks do not always reflect from the wall as shown in this example, however. To illustrate the reason why, let us revisit the example problem, but increase the wedge angle to 30°.

---

### 12.3.2 Numerical Example: Reflection of an Oblique Shock Wave in Mach 3 Flow Generated by 30° Wedge

**Problem:** Returning to the oblique shock in Section 12.3.1, increase the wedge angle to $\delta_1 = 30°$ and attempt to solve for the reflected shock.

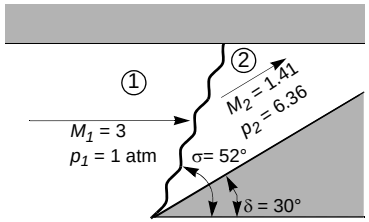


**Solution:** Solving for the flow behind the initial (referred to from now on as the *incident*) oblique shock does not present any problems. Using the method of Section 12.2.1, we can solve for the shock angle $\sigma = 52°$ and the flow behind the incident shock is at Mach 1.41. When this flow encounters the wall, it must turn back through a deflection angle of 30°. Herein lies the problem: for Mach 1.41, the maximum deflection angle is 9.7°. Thus, there is no reflected oblique shock solution at the wall that can match the flow condition required by the wall. What happens?

---

You might think this problem is similar to the problem of the wedge that exceeds the maximum deflection angle, as discussed in Section 12.2, and that a normal shock is formed at the wall. This is partially correct, but how does this normal shock at the wall match up with the incident shock originating from the $\delta_1 = 30°$ wedge? The result is a more complex flow pattern discussed in the next section.

## 12.4 Mach Reflection

The answer to the question "What happens when there is no oblique shock solution when a shock wave encounters a wall?" is that a pattern of three shocks appear: the incident shock, the reflected shock, and a third shock called the Mach stem. The reflected shock no longer emanates from the upper wall. Rather, the three shocks all meet at a point (called the *triple point*), with the Mach stem bridging the distance from the triple point to the upper wall. This Mach stem is usually a normal or nearly normal (strong oblique) shock that is, in general, slightly curved as it goes from triple point to the wall. The flow passing through this shock complex sees different states: the lower part of the flow passes through the incident oblique shock and the reflected shock (two shocks). The upper part of the flow passes through the single, strong Mach stem.

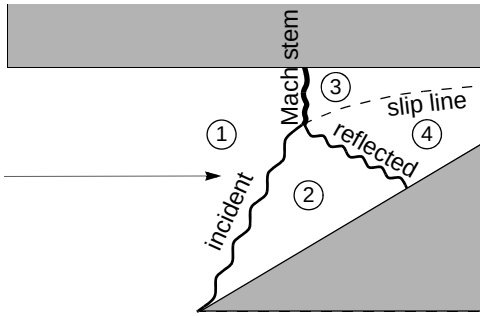


Because the upper and lower flows have a different shock history, they will in general have a different Mach number and velocity. Thus, there is a slip line emanating from the triple point that denotes the boundary between the gas that passed through the incident/reflected shock and the gas that passed through the Mach stem. Note that these two streams must have the same flow direction, however, and they must also match pressure. This is because the flows must be parallel (obviously, they cannot diverge and leave vacuum or pass through one another) and a slip line cannot support a discontinuity in pressure. Thus, we have two requirements:

$$\delta_2 - \delta_4 = \delta_3$$

$$p_3 = p_4$$

These two requirements turn out to be the key to determining the actual flow pattern observed.

This entire complex is called *Mach reflection*, in honour of Ernst Mach who discovered it in 1875. Interestingly, he discovered this phenomenon while studying unsteady shock waves (see Section 12.7) using a very "low tech" diagnostic method called a smoke foil (or soot plate): the passage of the triple point over a plate of glass that had been coated with soot left a distinct trace.*

---

*Krehl, P., and van der Geest, M. "The Discovery of the Mach Reflection Effect and its Demonstration in an Auditorium," *Shock Waves*, Volume 1, Number 1, March, 1991, pp. 3-15

It is believed the intense vorticity associated with the slip line emanating from the triple point rearranges the soot in the vicinity of the triple point.

## 12.5 Shock Polars

Because the flow downstream of a shock interaction such as a Mach reflection requires the flow directions and pressures match, it is convenient to plot the oblique shock relations we found in Section 12.2 in terms of the pressure ratio across the shock $\frac{p_y}{p_x}$ and the flow deflection angle $\delta$. Such a plot is called a *shock polar*. The shock polars are plotted here for Mach 2 to Mach 5 flow. These plot were constructed parametrically, by varying the shock angle $\sigma$ from $\alpha$ to 90° and then computing the deflection angle $\delta$ using Eq. 12.14 and the pressure ratio $\frac{p_y}{p_x}$ using Eq. 12.9. For a given Mach number and deflection angle, there are two possible shock pressures, corresponding to weak and strong oblique shocks, as discussed in Section 12.2. The shock polar curves have a turning point at the maximum deflection angle.

Shock polars are very useful graphical tools for determining the outcome of shock interactions, i.e., which shock patterns are actually observed.

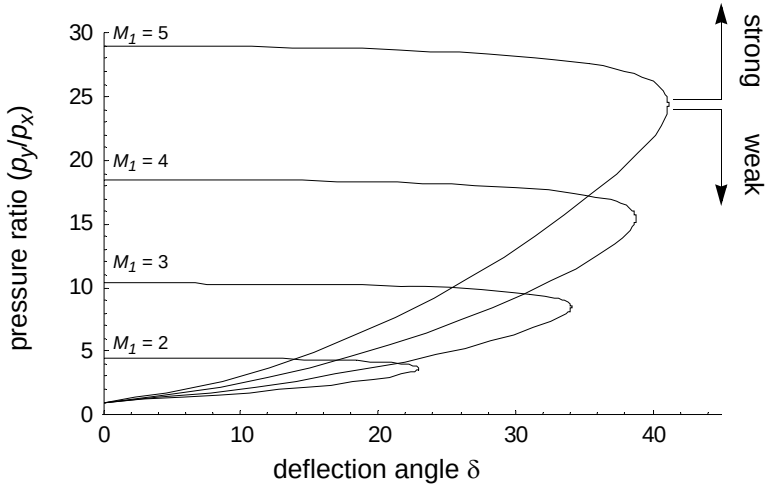


### 12.5.1 Regular Reflection via Shock Polars

Shock polars are helpful in deciding when regular reflection can occur and can be used to solve for the reflected shock in the case of regular reflection. To illustrate this point, let us return to the numerical example of Section 12.3.1 and plot the shock polar for the approaching Mach 3 flow. Since the flow downstream of the shock has been deflected by 10° and compressed to $2.055\,p_1$, we can plot a second polar that starts at that deflection angle and pressure. Note that the pressure ratio plotted for the second shock is $\frac{p_3}{p_1}$ (not $\frac{p_3}{p_2}$). This second polar is plotted with the flow deflection in the negative direction, since we know that the reflected shock is caused by the upper wall forcing the flow back down. We see the reflected shock polar intersects the *y*-axis, corresponding to a net deflection angle (with respect to the original flow direction) of 0°. This intersection point is the solution we are interested in: it is the reflected shock that will redirect the flow back to parallel with the upper wall. From the plot, we can see the pressure behind this second shock is $3.83\,p_1$, which agrees with what we found in Section 12.3.1. From this intersection point, we can also determine the other parameters for the reflected shock.

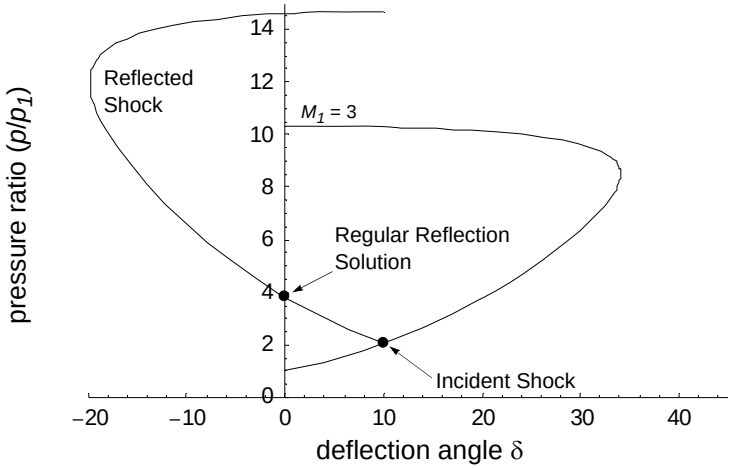

## 12.5.2 Mach Reflection via Shock Polars

We can also construct the shock polars for the case where we could not obtain a regular reflection, such as the example in Section 12.3.2. We can readily see from the shock polars that there is no reflected shock that can restore the flow to be parallel to the upper wall, since the reflected shock polar cannot reach the *y*-axis. Thus, we must have the case of Mach reflection, as discussed above. Recall that, in order for the three shock comprising the Mach reflection to come together, the pressure and net deflection angle of the flow leaving the reflected shock and Mach stem must be the same (i.e., $\delta_2 - \delta_4 = \delta_3$ and $p_3 = p_4$). Note that the shock polar for the incident shock is also the polar for the Mach stem, since they both see the same freestream flow approaching the wedge. Thus, the solution for the Mach reflection is the point where the two polars intersect.

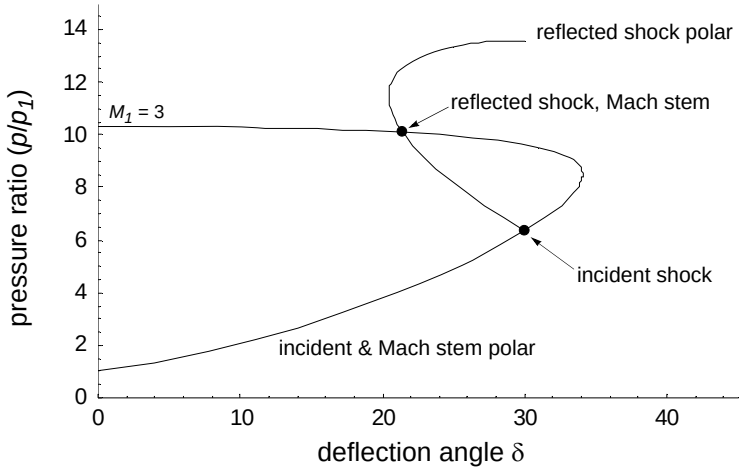


Knowing the deflection angle for the Mach stem ($\delta_3 = 21.4°$) and the deflection angle for the reflected shock ($\delta_4 = 8.6°$), the flow exiting the various shocks and the shock angles can readily be determined. The entire pattern of the triple point is reconstructed here.

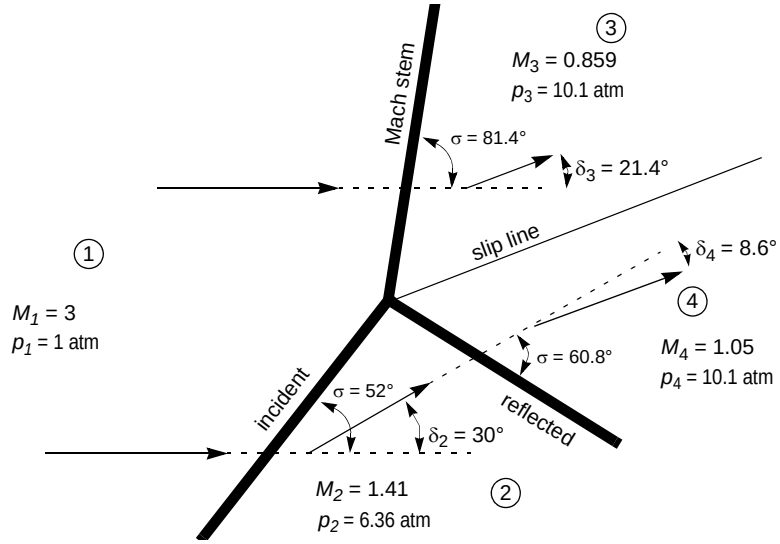


Note that the flow has not been deflected back to the freestream flow direction; it is still deflected upward with $\delta = 21.4°$. Thus, there must be additional turning of the flow before it reaches the upper wall. This results in both the Mach stem and the slip line curving. The flow downstream of the Mach stem is subsonic, so it can smoothly compensate to match the conditions demanded downstream by the wall and other boundaries. We can conjecture that the Mach stem is normal when it reaches the wall, so the flow is parallel to the wall, but we cannot easily solve for its shape. What is more, we do not know exactly where in the flow the triple point will position itself. Determining the entire flow pattern is extremely challenging and, in general, can only be achieved through computational fluid dynamics (CFD). However, we *do* know that when the three shock waves come together, the local flow pattern will be as is shown here, since this is the *only* permitted 3-shock solution for the initial flow and wedge angle.

Considering the geometry of the shock polars, some important conclusions can be made. For one, note that the only way a reflected shock polar can intersect the original shock polar is by crossing the upper, strong oblique shock solution. Thus, Mach stems are always *strong* oblique shocks. Further, the flow downstream of a Mach stem is always *subsonic* relative to the Mach stem. The reflected shock may have subsonic or supersonic flow exiting the wave.

## 12.6 Transition Criteria

The use of shock polars can determine the geometry and strength of shock waves when Mach reflection occurs, as discussed above. Shock polars can also be used to solve for regular reflection, as discussed in Section 12.5.1. Where a considerable amount of difficulty is encountered is in determining when the transition from regular reflection to Mach reflection occurs. This issue has not been entirely resolved, despite intensive study throughout the second half of the 20th Century.* In this section, we will examine some of the criteria that have been proposed to determine when the transition from regular reflection to Mach reflection occurs.

### 12.6.1 Detachment Criterion

An obvious suggestion, considering the polars we have examined so far, is that the transition to Mach reflection occurs when the reflected shock polar no longer intersects the *y*-axis. This condition is called "detachment" or "maximum deflection" criterion, since it occurs at the maximum deflection angle for the reflected oblique shock. In this case, there can be no regular reflection, and Mach reflection must occur. The critical case where detachment occurs for Mach 3 incident flow is shown here.

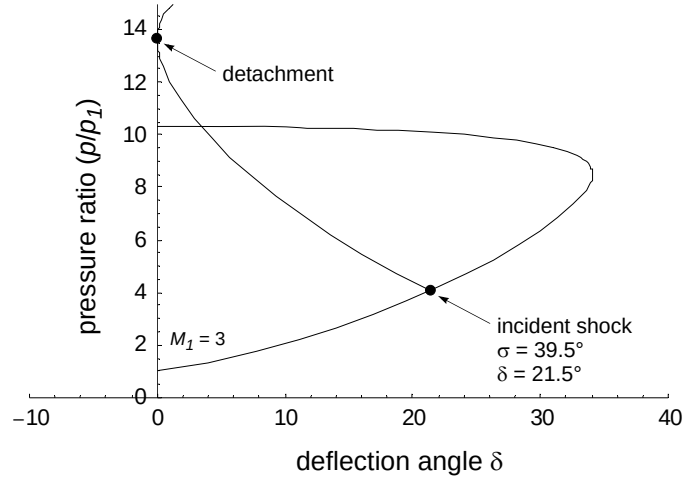


*A search with database services such as Compendex or Inspec will reveal that over 1000 scientific papers on the subject of the transition to Mach reflection have appeared since 1950!

### 12.6.2 Sonic Criterion

Another suggested criterion is that when the reflected shock in a regular reflection can "sense" the flow disturbances downstream, such as those generated from the walls of the channel downstream of the reflection point, it will transition to a Mach reflection. In other words, when the flow downstream of the reflected oblique shock becomes sonic, Mach reflection will occur.

As was pointed out in Section 12.2, the condition where flow becomes sonic downstream of an oblique shock is very, very close to the maximum deflection angle, particularly at high Mach numbers. Thus, in practice, the sonic criterion becomes very close to the detachment criterion (note that in our Mach 3 example, the difference in critical deflection and shock angle is only 0.2°). Experimentally differentiating the detachment criterion from the sonic criterion is very challenging.

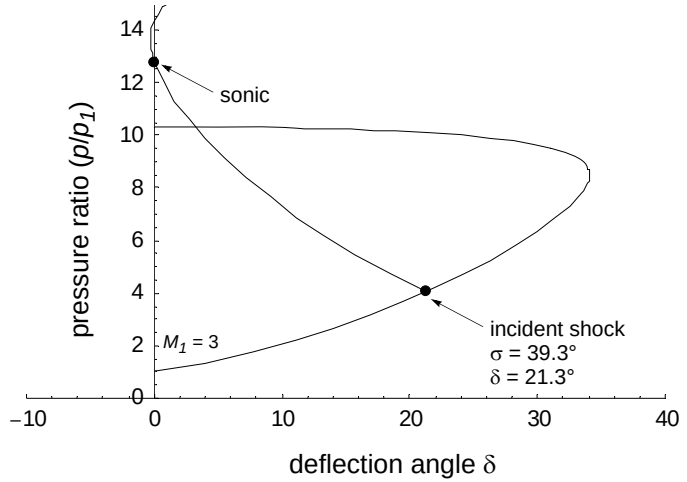

## 12.6.3 Mechanical Equilibrium Criterion

Yet another criterion for transition is that Mach reflection will occur when the reflected shock in a regular reflection also corresponds to a normal shock in a Mach reflection. In terms of shock polars, this condition means that the reflected shock polar intersects the *y*-axis at the same point as it intersects the incident/Mach stem polar. Mathematically, this condition can be expressed as: $\delta_2 - \delta_4 = \delta_3 = 0$. Thus, this condition corresponds to the case where either regular reflection or Mach reflection with a normal shock are valid solutions. This case is illustrated below.

This condition is called the "mechanical equilibrium" or "von Neumann" criterion. The latter name is in reference to John von Neumann, who wrote a seminal study on Mach reflection during the Second World War.* In fact, von Neumann also discussed the sonic condition as well. The idea behind this condition is that, as soon as the regular reflection point on the *y*-axis reaches the polar for the incident shock/Mach stem (recall, the incident shock and Mach stem share the same polar), Mach reflection becomes possible, and therefore will occur. In other words, *as soon as a Mach reflection solution with a normal shock exists, the transition to Mach reflection will occur.*

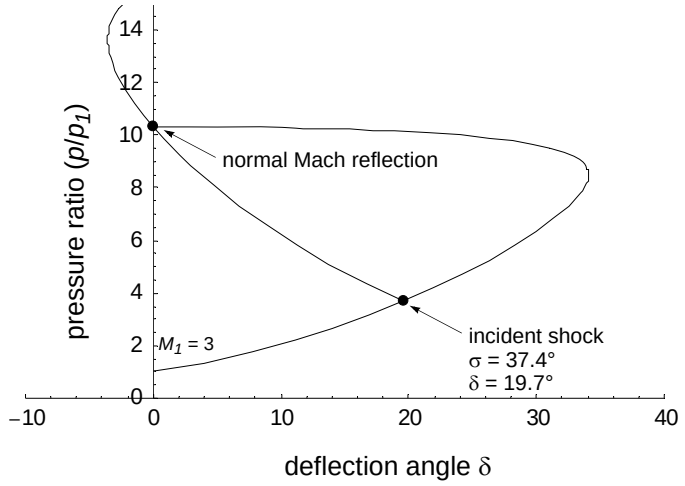


*von Neumann, J., "Refraction, Intersection, and Reflection of Shock Waves," NAVORD Report 203-45, Navy Dept., Bureau of Ordnance, Washington D.C. 1943, also: "Oblique Reflection of Shocks," Explos. Research Report 12, Navy Dept., Bureau of Ordnance, 1943.

## 12.6.4 Which Criterion to Use

Note that in the figures above, the critical incident shock angles (either shock angle $\sigma$ or deflection angle $\delta$) were found be somewhat different for the different criteria used (in the case of detachment vs. sonic, only very slightly different). To determine which of these suggested criteria is the correct one, we can examine a sequence of polars for Mach 3 flow where the incident shock angle is incrementally increased through five cases:

1. A case just below the mechanical equilibrium criterion
2. The mechanical equilibrium/von Neumann criterion
3. A case just above the mechanical equilibrium/von Neumann criterion
4. The sonic/detachment criterion (difference too small to resolve here)
5. A case just above the sonic/detachment criterion

For Mach 3 flow, this corresponds to increasing the deflection angle $\delta$ from 18.5° to 22.5° in roughly 1° increments. For cases where the reflected shock polar crosses the *y*-axis, the regular reflection solutions are labeled, *a*-*b*-*c*-*d*. For cases where the reflected shock and Mach stem shock polars intersect, the Mach reflection solutions are labeled *w*-*x*-*y*-*z*. Point *b* and *w* are actually the same point, since the mechanical equilibrium solution can correspond to either regular or Mach reflection.

Let us now consider the sequence of events if we were to slowly increase the wedge angle in a Mach 3 flow and vary the incident oblique shock from case 1 to case 5. In case 1, the only solution is regular reflection, so there is no issue. In case 2, the *mechanical equilibrium* solution would state that the transition to Mach reflection occurs. The mechanical equilibrium criterion predicts that as the incident shock angle is increased further, the Mach reflection points move to the right, following the sequence: *b*/*w*-*x*-*y*-*z*.

If the detachment criterion (or sonic) is used, then as the oblique shock angle increases, the regular reflection solution continues to be the predicted solution, until the sonic/detachment condition occurs in case 4. For case 5, only Mach

reflection can occur, so there is no ambiguity regarding this case. Thus, the sequence of solutions predicted by the detachment criterion is: *a-b-c-d-z*. Note that there is an abrupt jump from point *d* to point *z*. The pressure behind the shock complex would abruptly drop from 13.6 atm down to 10.3 atm as the incident shock angle is increasing (or an abrupt jump up in pressure if the original wedge angle is decreasing). This counterintuitive behavior is often used as grounds to reject the sonic/detachment criteria in favor of the mechanical equilibrium/von Neumann criterion.

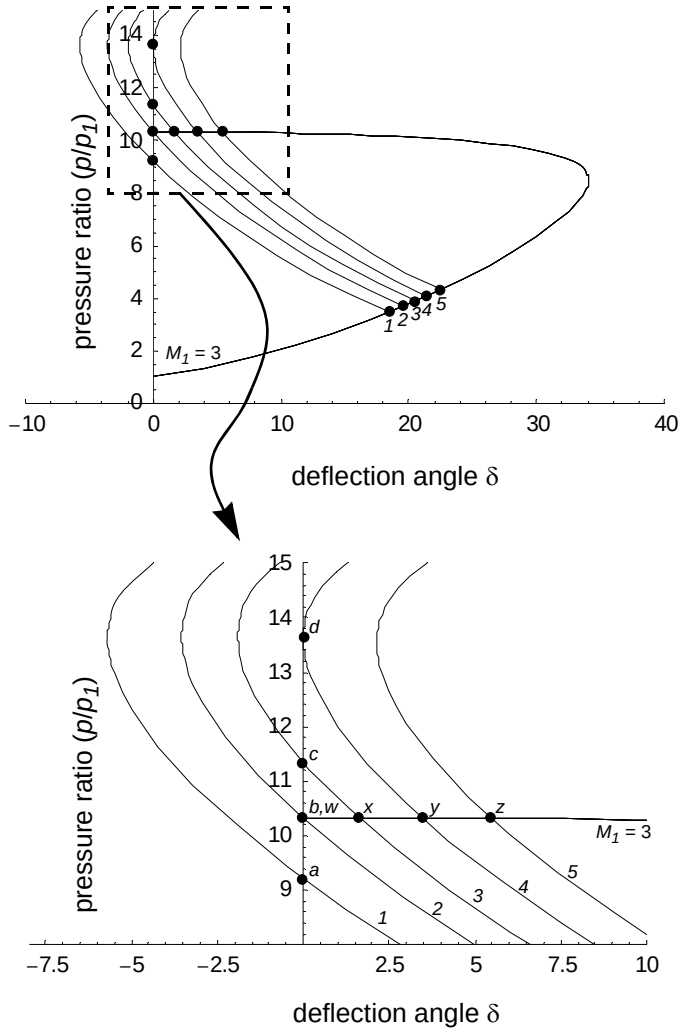


Note that the mechanical equilibrium/von Neumann criterion gives a continuous variation in pressure and flow direction as the transition from regular reflection to Mach reflection is made. The name "mechanical equilibrium" reflects this aspect of the criterion, since the pressure behind the reflection point varies smoothly as the shock angle is changed.

Extensive experimental investigation has not been able to identify a single transition criterion. Some experimental results are consistent with the detachment criterion, others with the mechanical equilibrium criterion. The current understanding is that both flow patterns (regular reflection and Mach reflection) may be observed in conditions in between the predicted transition criteria, depending on the details of the flow (history of the flow, disturbances, etc.).

We can repeat the calculations and shock polar constructions we performed above for a range of Mach numbers and plot the various transition criteria. This is done in the figure shown below, where the critical shock angles $\sigma$ for the detachment and mechanical equilibrium criteria are plotted as a function of Mach number. The Mach angle $\alpha$ is also plotted (the minimum angle an oblique shock can have).

The figure should be interpreted as follows: for shock angles greater than the detachment criterion curve, *Mach reflection must occur.* For shock angles less than the mechanical equilibrium criterion, *regular reflection must occur.* Between the two curves, *either Mach reflection or regular reflection can occur.* The situation is qualitatively similar to the problem of starting a supersonic inlet, as discussed in Section 9.2. Recall that, between the starting limit where the normal shock is swallowed by the inlet and the isentropic limit, a supersonic inlet can be either started or unstarted. This fact resulted in a hysteresis phenomenon: the inlet could have either subsonic flow or supersonic flow for the same area ratio and flight Mach number, depending on the history of the flow up to that point. Recent results obtained in the last 15 years suggest a similar hysteresis can occur in Mach reflection: as the shock angle is slowly increased, regular reflection can continue to occur up until the detachment criteria is reached (point *d*) and an abrupt transition to Mach reflection occurs. If the shock angle is then decreased, the Mach reflection

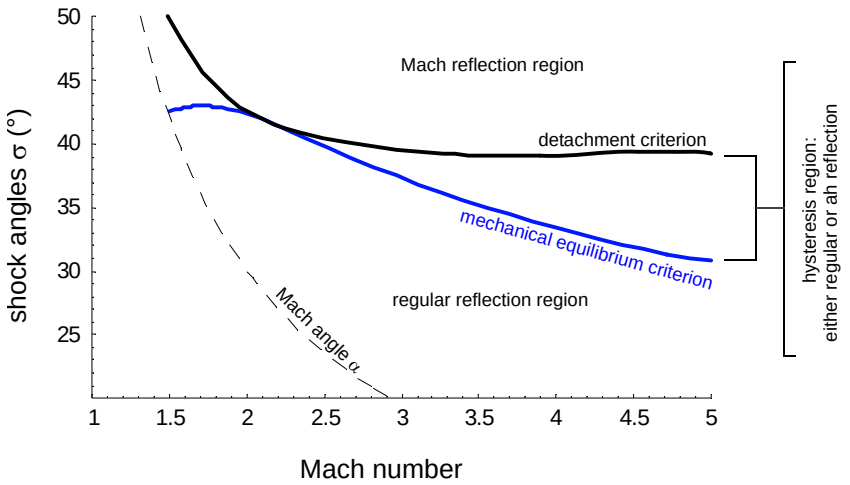


persists until the mechanical equilibrium criterion is satisfied (point b,w), and transition back to regular reflection occurs. A similar hysteresis can occur with variations in Mach number as well.

This phenomenon has been observed both experimentally and computationally. However, different results have been obtained in different experimental facilities, depending on subtle details of the apparatus (for example, in tests performed in supersonic wind tunnels, different results have been observed depending on whether the test section is closed or an open "jet" type wind tunnel). This suggests that the transition criterion is sensitive to disturbances in the flow.

Note that around Mach 2.2, the curves intersect, and below about Mach 1.5, the mechanical equilibrium criterion crosses the Mach angle. What happens in these regimes requires further consideration and will not be discussed here (see Section 12.8: Caveats).

## 12.7 Mach Reflection in Unsteady Flow

Mach reflection also occurs in unsteady flows as well. In fact, Mach reflection has been much more extensively studied in unsteady flows than in steady flows, owing to the simplicity of the experiment apparatus required to explore unsteady flows (essentially, just a shock tube).

### 12.7.1 Mach Reflection of a Shock Passing a Wedge

The most frequently studied example of Mach reflection is when a normal shock wave encounters a wedge, as illustrated here. Recall that in the lab-fixed reference frame, unsteady shock waves accelerate the flow in the direction of shock propagation. Thus, there is a flow induced behind the normal shock. While the incident shock runs up the wedge, flow behind it cannot flow through the wedge. Thus, a reflected shock forms that propagates back into the shock-accelerated gas, deflecting it as demanded by the surface of the wedge.

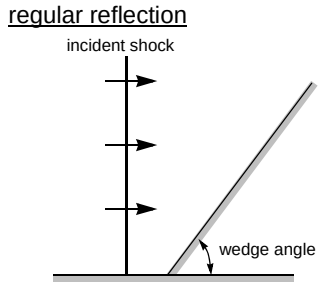


For very large wedge angles, the shock is reflected from the wedge at the wedge surface (regular reflection).

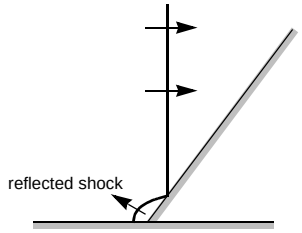


For smaller wedges, the reflection occurs as a Mach reflection, with a Mach stem propagating nearly normally up the wedge surface, as shown below. Note also the appearance of a slip line denoting the boundary between the gas that was processed by both the incident and reflected shock wave and the gas that passed through the normal shock. The Mach stem in this case grows linearly as it propagates up the wedge; the trajectory of the triple point is shown as a dashed line.

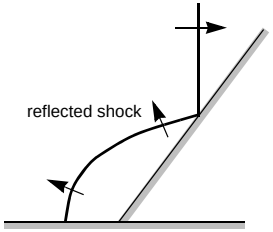

Based off our development of Mach reflection in steady flows in the last section (Sections 12.5-12.6), it may be confusing that Mach reflection occurs with *smaller* wedge angles in unsteady flow, while it occurred with *larger* wedge angles in steady flow. However, the wedge is playing a different role in these two different flows. In steady flow, increasing the wedge angle steepened the shock with respect to the flow (i.e., the shock angle increases), approaching the region where the maximum deflection angle occurs upon reflection. In an unsteady flow, it is convenient to transform into the reference of the reflection point (triple point, in the case of Mach reflection). In this reference frame, a wedge of larger angle means the incident shock is not as steeply inclined to the flow approaching the shock (i.e., the shock angle is smaller), and thus Mach reflection is less likely to occur. For a shallow wedge, the incident shock is already nearly normal to the flow in the reference frame of the reflection point, making Mach reflection more likely.

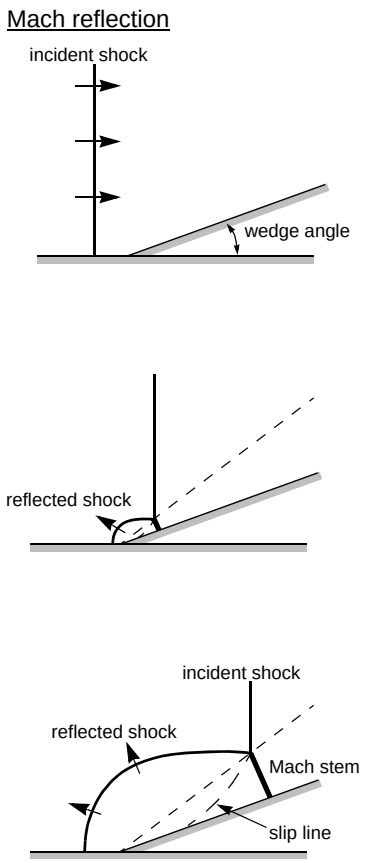


The use of a reference frame attached to the reflection point is widely utilized in studying unsteady shock reflection, since it can render an unsteady flow effectively steady in the new reference frame. In the case of the shock-wedge interaction, the resulting flow is nearly self-similar, meaning that drawings of the shock geometries shown above are, at later time, just photo-enlargements of the same shock geometry from earlier time. Similarity would mean that the Mach stem grows linearly with time and the triple point trajectory is a straight line. These predictions are not always verified exactly in experiments, but the flow is nearly self-similar enough to make this approach worthwhile. Using the reference frame of the triple point to render the flow pattern fixed is referred to as *pseudosteady flow.*

The analysis of shock reflection in unsteady or pseudosteady flow follows the same treatment invoking shock polars and detachment criteria as discussed in treating steady flow. The complications arise in accounting for the more widely varied flow patterns observed in unsteady shock reflection experiments as compared to steady shock reflection. As an example, a more complicated reflection is illustrated here, called double Mach reflection, in which a second triple point occurs on the reflected shock behind the first triple point, with its own Mach stem, slip line, etc.

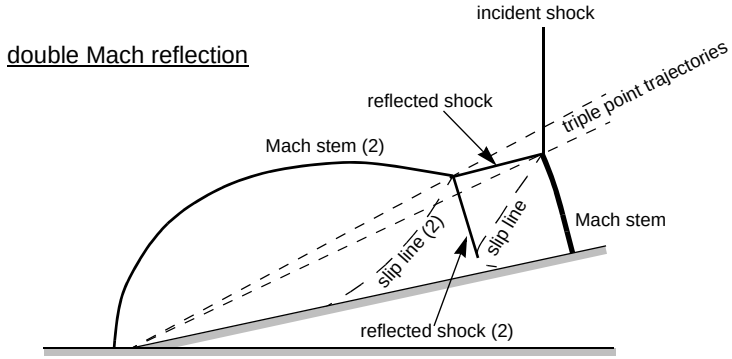


## 12.7.2 Mach Reflection in Interacting Blast Waves and Blast Reflection

Mach reflection occurs in other unsteady flows, such as the interaction of blast waves or reflection of blast waves from a rigid wall. Blast waves are shock waves that originate from a concentrated (point-like) source, such as an explosion. Blast waves are still shock waves and all our shock relations are still valid. However, since the source driving the shock wave (such as the detonation of a charge of high explosive) decreases in its ability to drive the shock, the shock wave decays in velocity as it expands outward. Such unsteady, decaying shock waves are called blast waves; the resulting flowfields cannot be rendered steady over their entire duration by a simple Galilean transformation.

When a blast wave encounters a rigid surface, such as the ground under an air burst, the leading front of the blast is usually normal to the surface, and reflects as a normal shock. As the curved portions of the blast front encounter the wall, the angle between the shock wave and the wall steadily increases. Eventually, the blast front becomes nearly perpendicular to the wall, and Mach reflection must occur. If the local interaction of the blast front with the rigid surface is examined, it is similar to the shock-wedge problem discussed in the prior section (Section 12.7.1). The additional complication is that the flow cannot be rendered steady or pseudosteady via a simple coordinate transformation; blast wave flow fields are irreducibly unsteady. Again, a variety of intricate shock patterns can be seen in Mach reflections observed and some surprising behavior noted. For example, the pressures generated on the ground by a blast in the atmosphere may be greater at points further from the point directly under the blast (ground zero), where Mach reflection occurs, rather than nearer to ground zero, where regular reflection occurs, even though the incident shock has decayed in strength by the time it reaches the farther point.*

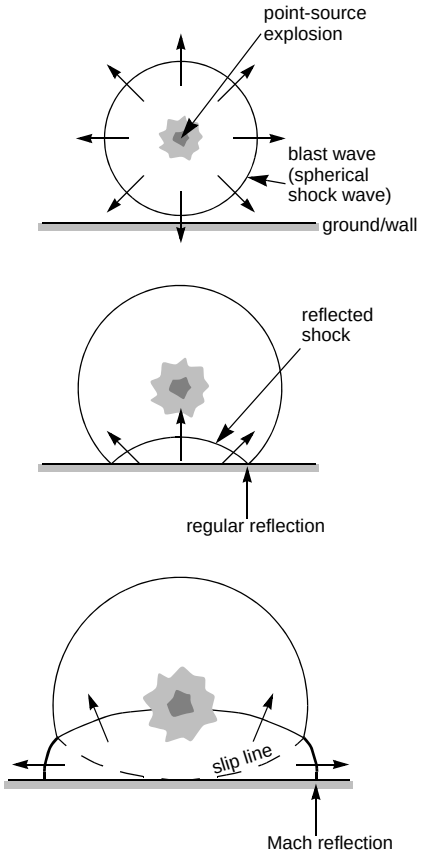


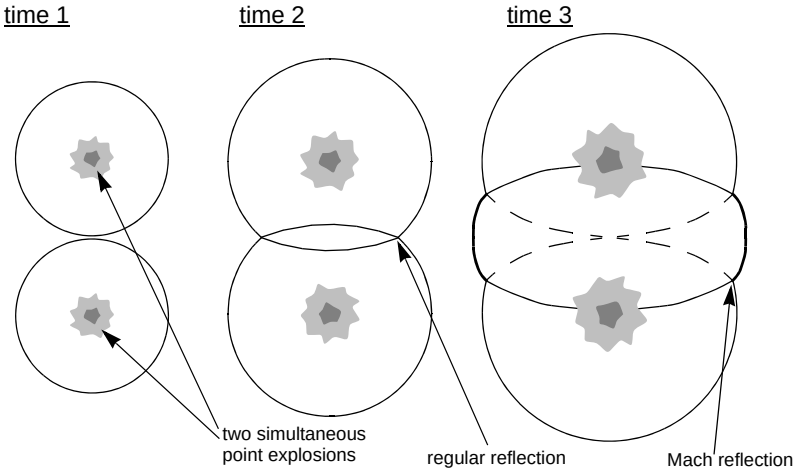


Essentially the same reflection phenomenon occurs when two blast waves intersect each other. This interaction was how Ernst Mach originally discovered the phenomenon while studying the blast waves generated by to simultaneous near-by spark discharges. The interaction of blast waves sounds like an unlikely scenario requiring study, however, detonation wave fronts in explosive gases (e.g., hydrogen-air, propane-oxygen, etc.) are comprised of an ensemble of interacting blast waves that propagate back and forth across the detonation front, resulting in detonation wave fronts having a roiling, cellular structure. The presence of Mach reflection, particularly the reflected shock

schlieren picture of detonation wave in methane/oxygen at low pressure

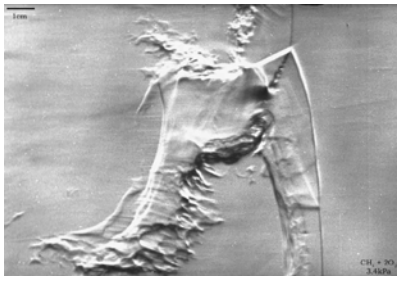

Photo: Matei Radulescu, McGill University

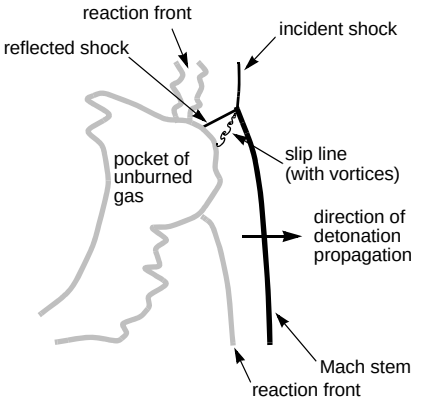


*These issues simulated considerable research into optimal "Height of Burst" effects during the 1950's and 1960's, when the large budgets of the Cold War were available to investigate means to optimize the destructive force of nuclear weapons.

and slip lines, in the shock interactions that comprise detonation waves are now believed to play a role in the actual burning of the explosive gas within the detonation front. The photograph here shows an extremely close-up side view of a detonation in methane/oxygen. The Mach reflection triple point and slip line (with vortices rolling up) is clearly visible. The reason why detonation waves have such complicated structures is an active area of research.

## 12.8 Caveats

This chapter can provide only the briefest introduction to the phenomenon of Mach reflection. The array of phenomena observed in Mach reflection studies can be bewildering, and research in the field takes on some of the attributes of taxonomy: inverse Mach reflection, transitional Mach reflection, negative double Mach reflection, von Neumann reflection, to name a few of the types of Mach reflections that have been observed. Collectively, these are referred to as *irregular reflection*, to contrast them with the well defined, two-shock regular reflection. Mach reflection has been studied in gases as varied as helium ($\gamma = 1.666$) to sulfur hexafluoride ($\gamma = 1.1$), in dusty gases, for wedges with rough surfaces or made from soft foam, for shock waves in gases reflecting *off* water, for shock waves *in* water reflecting off steel, even for shock waves in plasmas! Researchers studying these phenomena present and compare their results at periodic International Mach Reflection Symposia.

In general, predicting Mach reflection phenomenon becomes more complicated for weaker shock waves, as alluded to in Section 12.6.4. For shock Mach numbers less than about Mach 1.5 (for $\gamma = 1.4$), there exists shock angles for which neither regular nor Mach reflection solutions can be found: the reflected polar does not intersect either the *y*-axis or the incident/Mach stem polar at all. This problem was given a somewhat melodramatic title "The von Neumann Paradox."

In the numerical examples of this chapter, we were careful to examine high Mach number flows (Mach 3) to avoid these issues associated with weaker shock waves.

Readers interested in the answers to these questions or further study into Mach reflection in general would benefit from consulting these review papers/book written by the leading researchers in the Mach reflection field:

- Ben-Dor, G., "Oblique Shock Wave Reflections" *Handbook of Shock Waves*, G. Ben-Dor, O. Igra, T. Elperin, eds., Academic Press, 2001.
- Ben-Dor, G., *Shock Wave Reflection Phenomena*, Springer-Verlag, 1992.
- Ben-Dor, G., "Steady, Pseudo-Steady, and Unsteady Shock Wave Reflections," *Progress in the Aerospace Sciences*, Vol. 25, 1988, pp. 329-412.
- Hornung, H., "Regular and Mach Reflection of Shock Waves," *Annual Review of Fluid Mechanics*, Vol. 18, 1986, pp. 33-58.

These caveats should never distract from the fact that the normal and oblique shock relations are always valid for shock waves in gases, and that all shock waves can be locally rendered steady via a coordinate transformation. What is more, if Mach reflection occurs, the solution identified for the reflected shock and Mach stem at the triple point is the correct one, matching experiments reasonably well, and likewise for regular reflection. The contentious issues only arise when determining when the transition from regular reflection to Mach reflection occurs. For many engineering calculations, simply assuming the mechanical equilibrium or detachment criteria may be entirely sufficient (or, calculations can be performed with both assumptions to bound the expected phenomenon). In short, never be afraid to apply the oblique shock relations or construct a shock polar. We may not be able to solve the entire flow field, but we can often obtain the information we need from simple application of shock relations and polars.

# 13.Prandtl-Meyer Expansion Flow

This chapter will treat flow over a expansive corner, i.e., one that turns the flow outward. But before we consider expansion flow, we will return to consider the details of the compressive corner case that results in oblique shock waves (the topic of Chapter 12). If we zoom in to examine a corner that is not a perfectly sharp edge, but rather a corner with a finite radius of curvature:

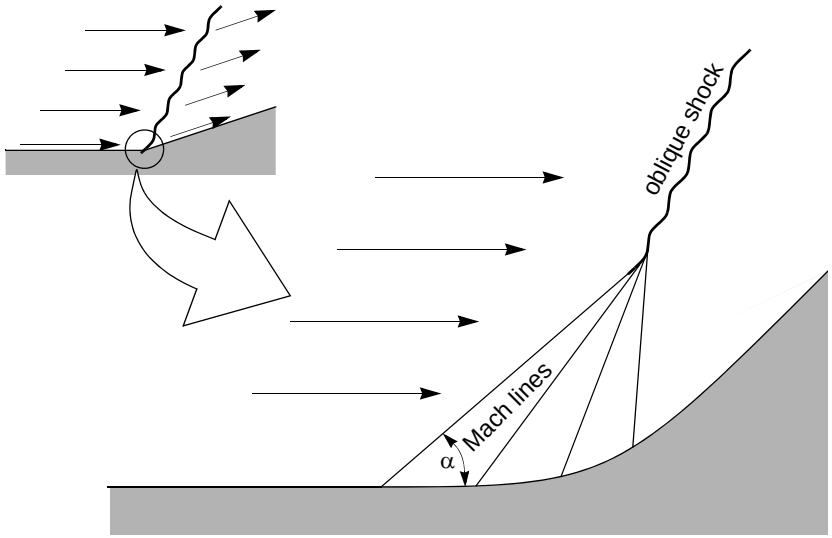


we see that the oblique shock is not formed instantaneously. Rather, the first disturbance created at the corner propagates outward from that point as a Mach line at angle $\alpha = \sin^{-1}\frac{1}{M}$. This is not a shock wave, but rather a weak disturbance that communicates the presence of the corner to the flow. This is followed by other disturbances which also propagate at the local Mach angle. Because the prior disturbances have deflected the flow upward and compressed the flow (decreasing the Mach number and, thereby, increasing the Mach angle), the later disturbances will be at a greater angle with respected to the horizontal than the original disturbance. Thus, the later disturbances tend to overtake the earlier ones. When these disturbances merge together, an oblique shock with a finite jump in pressure, velocity, etc., is formed. Thus, even if a corner is locally gradual with a finite radius, an oblique shock will eventually form. The shock angle and other properties of this oblique shock will be the same as if the original corner was sharp and discontinuous. This is the two-dimensional, steady analog of the generation of a normal shock by the gradually accelerating piston discussed in Section 7.1; note the similarity between the drawing here and the *x-t* diagram of the accelerating piston generation of a shock in Chapter 7.

Examining the analogous flow over an expansive corner, we see that the successive Mach lines tend to have a smaller slope, due to the changing angle of the flow and the increasing Mach number as the flow expands (resulting in a decreasing Mach angle). Thus, these disturbances can never coalesce together to form a shock, and the flow remains isentropic. Similar to how a piston that is rapidly extracted from a cylinder generates a rarefaction wave, the flow over

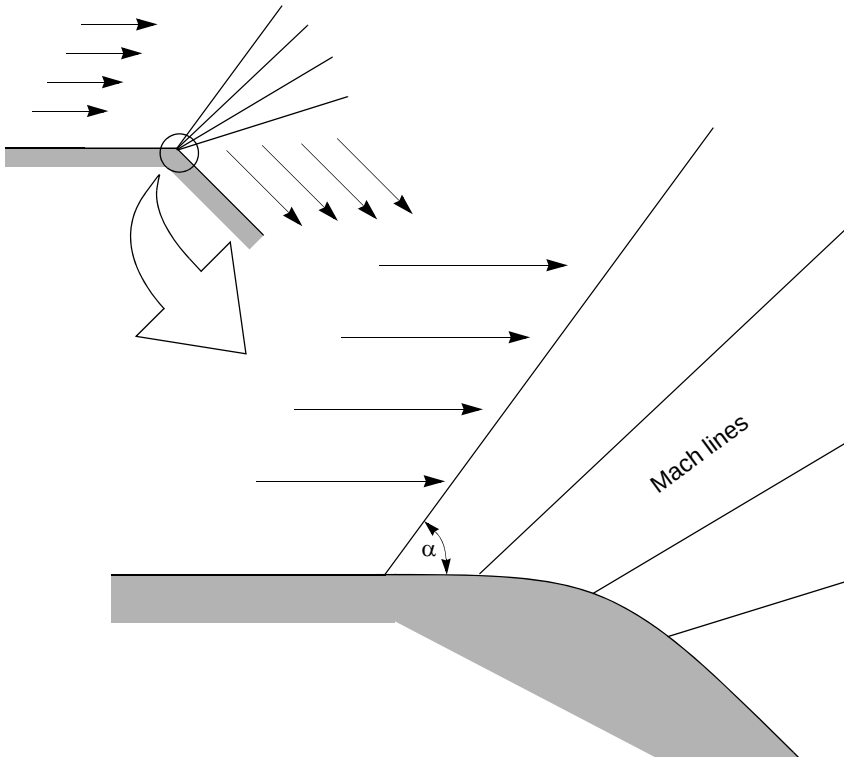

an expansive corner generates an expansion fan. If the corner is sharp, the resulting flow is called a *centered Prandtl-Meyer expansion fan*. The analysis developed in this chapter applies to any uniform supersonic flow that encounters a gradual area change, as long as the disturbances do not coalesce into a shock. Thus, the analysis is valid for the initial stages of flow over a gradual compressive corner, and is valid for the entire flow over an expansive corner.

## 13.1 Working Relations for Prandtl-Meyer Flow

We begin by considering a single disturbance wave generated by a slight deflection of the wall:

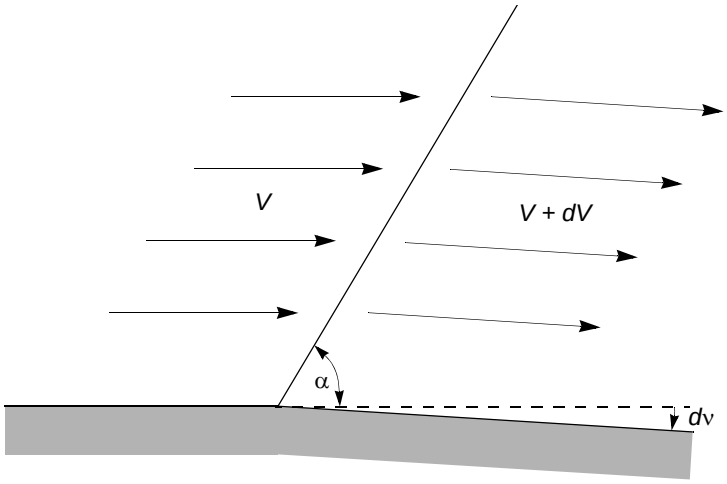


The flow is deflected downward by an angle $d\nu$.

The disturbance wave is at an angle $\alpha = \sin^{-1}\frac{1}{M}$ with respect to the approaching flow. We can interpret this relation for the Mach angle via the triangle shown here. From this triangle, we can find relations for $\cos\alpha$ and $\tan\alpha$:

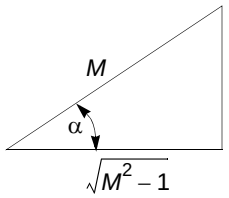


$$\cos\alpha = \frac{\sqrt{M^2-1}}{M}$$

$$\tan\alpha = \frac{1}{\sqrt{M^2-1}}$$

These will be useful in our development.

Superimposing the velocity vectors for the flow coming into and out of this wave:

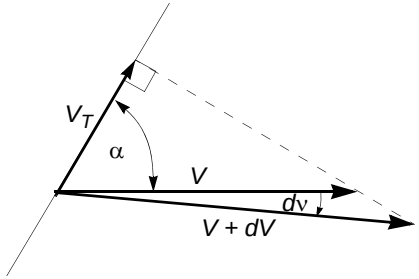


Note that the tangential component for the velocity vector upstream and downstream of the wave must be equal, as dictated by the momentum equation (review Section 12.2 if this point is unclear). The tangential component of velocity is related to the resultant velocity by:

$$\frac{V_T}{V} = \cos\alpha$$

By using our previous expression for $\cos\alpha$:

$$\frac{V_T}{V} = \cos\alpha = \frac{\sqrt{M^2-1}}{M} \Rightarrow V_T = V\frac{\sqrt{M^2-1}}{M}$$

Likewise, for the velocity downstream of the wave:

$$\frac{V_T}{V+dV} = \cos(\alpha + d\nu)$$

Expanding $\cos(\alpha + d\nu)$:

$$\cos(\alpha + d\nu) = \cos\alpha\cos d\nu - \sin\alpha\sin d\nu$$

Since the deflection angle $d\nu$ is very small ($d\nu << 1$):

$$\cos d\nu \approx 1\,,\ \sin d\nu \approx d\nu$$

Thus:

$$\frac{V_T}{V + dV} = \cos\alpha - d\nu\sin\alpha$$

Using our expressions for $V_T = V\frac{\sqrt{M^2-1}}{M}$, $\sin\alpha$, and $\cos\alpha$:

$$\frac{V}{V + dV}\frac{\sqrt{M^2-1}}{M} = \frac{\sqrt{M^2-1}}{M} - \frac{1}{M}d\nu$$

Expanding $\frac{V}{V + dV}$ by long division:

$$\frac{V}{V + dV} = 1 - \underbrace{\frac{dV}{V} + \left(\frac{dV}{V}\right)^2 - \left(\frac{dV}{V}\right)^3 + \ldots}_{\text{H.O.T.}}$$

Since $\frac{dV}{V} << 1$, we can neglect the higher order terms. Thus:

$$\left(1 - \frac{dV}{V}\right)\frac{\sqrt{M^2-1}}{M} = \frac{\sqrt{M^2-1}}{M} - \frac{1}{M}d\nu$$

Simplifies to:

$$\frac{dV}{V} = \frac{1}{\sqrt{M^2-1}}d\nu$$

Or:

$$d\nu = \sqrt{M^2-1}\frac{dV}{V}$$

This differential relates the deflection angle $d\nu$ to the change in velocity $dV$ as a function of Mach number. Note that a positive $d\nu$ results in a positive $dV$, verifying our initial assumptions in the sign of $d\nu$ and $dV$. This agrees with our experience from one-dimensional isentropic supersonic flow: a diverging area should result in an increase in velocity.

We would like to integrate this relation for finite changes in angle, but we need to express the $\frac{dV}{V}$ term in terms of Mach number for this expression to be integrable. Starting with the definition of Mach number ($V = Mc$) and using logarithmic differentiation:

$$\frac{dV}{V} = \frac{dM}{M} + \frac{dc}{c}$$

Since the flow is adiabatic, we can relate the sound speed to the temperature:

$$\frac{c_o}{c} = \sqrt{\frac{T_o}{T}} = \left(1 + \frac{\gamma-1}{2}M^2\right)^{\frac{1}{2}}$$

$$c = c_o\left(1 + \frac{\gamma-1}{2}M^2\right)^{-\frac{1}{2}}$$

Differentiating:

$$\frac{dc}{c} = -\frac{\gamma-1}{2}M\left(1 + \frac{\gamma-1}{2}M^2\right)^{-1}dM$$

Thus, we can express $\frac{dV}{V}$ entirely in terms of Mach number:

$$\frac{dV}{V} = \left(1 - \frac{\frac{\gamma-1}{2}M^2}{1+\frac{\gamma-1}{2}M^2}\right)\frac{dM}{M} = \left(\frac{1}{1+\frac{\gamma-1}{2}M^2}\right)\frac{dM}{M}$$

So, our expression for $d\nu$:

$$d\nu = \left(\frac{\sqrt{M^2-1}}{1+\frac{\gamma-1}{2}M^2}\right)\frac{dM}{M}$$

can be integrated for a finite deflection of the flow:

$$\int_{\nu_1}^{\nu_2} d\nu = \int_{M_1}^{M_2} \frac{\sqrt{M^2-1}}{1+\frac{\gamma-1}{2}M^2}\frac{dM}{M}$$

Integration yields:

$$[\nu]_{\nu_1}^{\nu_2} = \left[\sqrt{\frac{\gamma+1}{\gamma-1}}\tan^{-1}\sqrt{\frac{\gamma-1}{\gamma+1}(M^2-1)} - \tan^{-1}\sqrt{M^2-1}\right]_{M_1}^{M_2}$$

Since this function is somewhat cumbersome, it is convenient to choose a reference angle for $\nu$. Defining $\nu_1 = 0$ at $M_1 = 1$, we obtain the *Prandtl-Meyer Function*:

$$\boxed{\nu = \sqrt{\frac{\gamma+1}{\gamma-1}}\tan^{-1}\sqrt{\frac{\gamma-1}{\gamma+1}(M^2-1)} - \tan^{-1}\sqrt{M^2-1}}$$

This function represents the angle $\nu$ that an initially sonic flow (i.e., flow starting at Mach 1) has been turned through to reach Mach number $M$. This

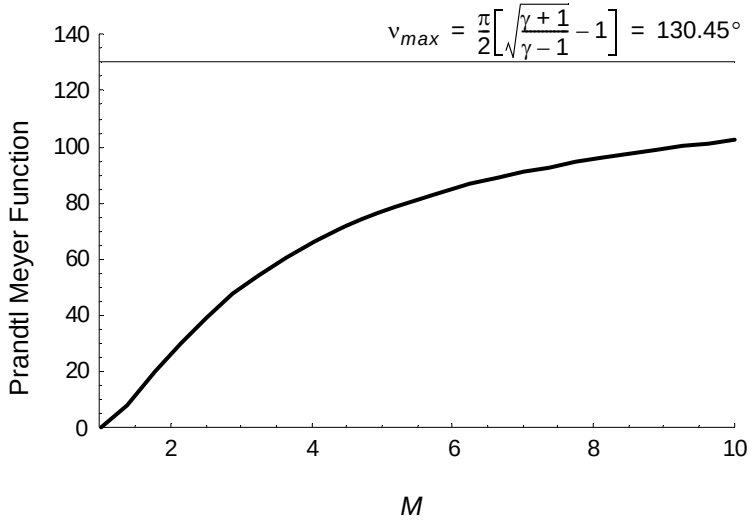


function is plotted here; tabulated values of $\nu$ as a function of $M$ can be found in Table A-6.

Note that in the limit as $M \to \infty$, the Prandtl-Meyer function $\nu$ reaches an asymptote:

$$\lim_{M\to\infty} \nu = \frac{\pi}{2}\left[\sqrt{\frac{\gamma+1}{\gamma-1}} - 1\right] = 130.45° \text{ (for } \gamma = 1.4\text{)}$$

Thus, flow that starts out sonic cannot be turned more than 130.45°. At this angle, the flow is fully expanded and the pressure and temperature decrease to zero. What happens if we try to force flow to turn though a larger angle by using a deflection angle greater than 130.45°? The flow can no longer follow the wall and, in principle, a region of vacuum exists between the maximum turning angle and the wall.*

*In a real experiment with real gases, the ideal gas law and calorically perfect gas assumptions break down as the temperature and pressure approach zero. In practice, a flow cannot reach the ideal maximum turning angle predicted from theory.

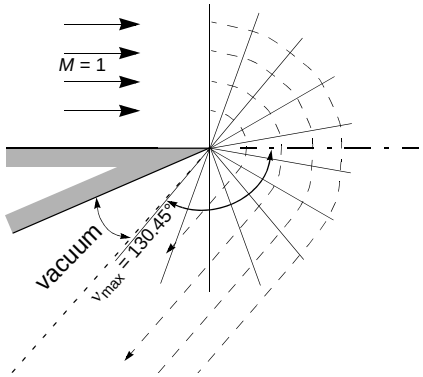


How do we use this function when we are considering a flow that does not originate at sonic conditions? This is best illustrated by a numerical example.

## 13.1.2 Numerical Example: Prandtl-Meyer Expansion

**Problem:** A supersonic flow at Mach 2 and 1 atm static pressure encounters a corner with a 10° expansion angle. Find the Mach number and pressure of the flow downstream of the corner.

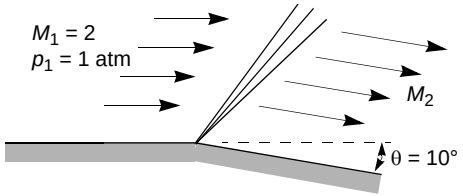


**Solution:** The solution technique is to consider that the flow originated at Mach 1 where the Prandtl-Meyer angle was 0°. The flow must then have been turned through $\nu_{M=2} = 26.38°$ in order to reach Mach 2.

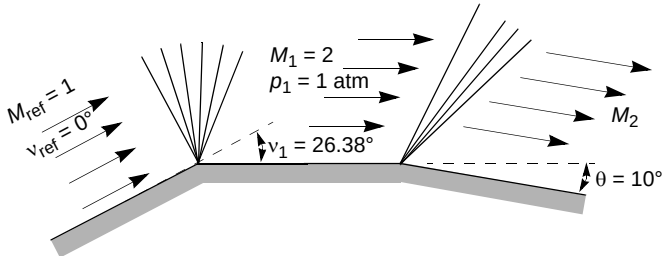


Thus, the flow approaching the corner in our problem has a value of $\nu = 26.38°$ associated with it. After it has been deflected an additional 10° by the corner, the new value of $\nu$ must be:

$$\nu_2 = \nu_1 + \theta$$

$$\nu_2 = 26.38° + 10° = 36.38°$$

Knowing the new value of the Prandtl-Meyer function, we can find the Mach number of the flow downstream of the corner:

$$\nu_2 = 36.38° \Rightarrow M_2 = 2.385$$

Since the flow is isentropic, we can use isentropic relations to find the pressure downstream of the corner:

$$\frac{p_2}{p_1} = \left(\frac{p_2}{p_o}\right)_{M_2}\left(\frac{p_o}{p_1}\right)_{M_1} = (0.0700)\left(\frac{1}{0.12780}\right) = 0.5477$$

Thus, $p_2 = 0.5477$ atm.

# 14. Applications of Oblique Shocks and P-M Expansions

## 14.1 Converging-Diverging Nozzle

Now that we are equipped with the relations for oblique shocks and Prandtl-Meyer expansions, we can return to the problem of the converging diverging nozzle with flow exhausting into a chamber with variable back pressure and resolve what happens in the cases of $p_4 > p_{back} > p_{design}$ and $p_{back} < p_{design}$ (recall Section 8.2). In other words, what happens when the back pressure is sufficiently low such that the flow chokes at the throat and becomes supersonic in the diverging section, but an isentropic flow or a combination of one-dimensional isentropic and normal shock flow cannot match the back pressure?

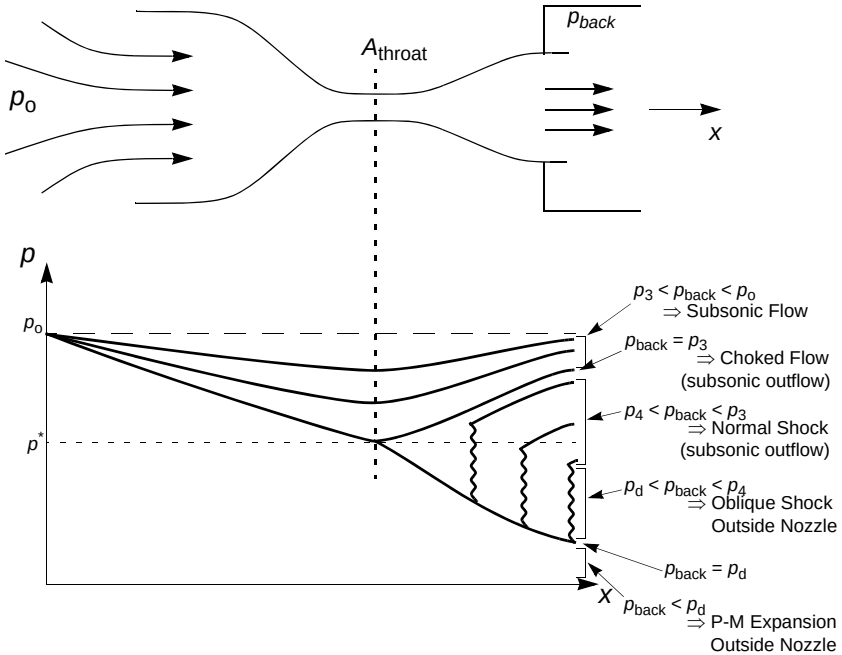


In the case where $p_4 > p_{back} > p_{design}$, the flow through the entire nozzle is supersonic, but the exit pressure (which will equal $p_{design}$) is less than the back pressure. The pressure mismatch is not enough to force a normal shock into the nozzle. In this case, an *oblique shock* will appear in the exhaust flow beyond the end of the nozzle. The oblique shock will be attached to the nozzle lip, and deflects the exit flow inward. The strength of the oblique shock will be such that the pressure after the shock matches the back pressure.

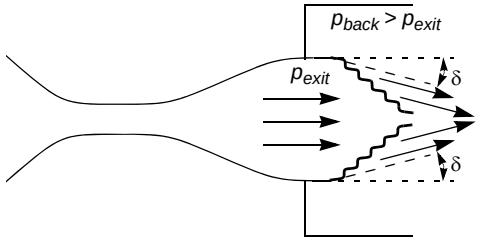


In the case of $p_{back} < p_{design}$, the nozzle flow is again entirely supersonic, but in this case the exit pressure (which will equal $p_{design}$) is greater than the back pressure. The flow, as it exits the nozzle, will further expand outward to match the ambient pressure via a *centered Prandtl-Meyer expansion fan* that is attached to the nozzle lip.

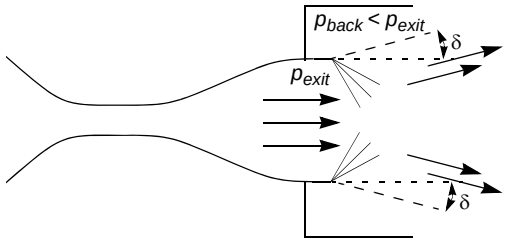


These exit flow phenomena show up in rocket nozzle exhaust plumes if the exit pressure does not exactly match the ambient pressure. If a rocket nozzle has been optimized for operation at sea level and then is operated at altitude, the resulting nozzle flow is *underexpanded*. The supersonic flow exiting the nozzle is at a higher pressure than the ambient pressure (which plays the role of back pressure). Thus, the flow will expand outwards via a Prandtl-Meyer expansion attached to the nozzle lip. If the mismatch in pressure is large, the

Lift-Off

At High Altitude

The Saturn I rocket, showing the exhaust plume from the nozzle at lift-off and when operating at high altitude. When at high altitude (low ambient pressure), the nozzle exhaust is *underexpanded*, resulting in the flow turning though a large deflection upon exiting the nozzle via a Prandtl-Meyer expansion.

Space Shuttle Main Engine

Tornado Jet Fighter

Overexpanded exhaust flow exhibiting Mach diamonds as a result of oblique shock waves in nozzle flow.

turning angle can be spectacular, approaching 90° or even greater. A photograph of a rocket (the Saturn I launch vehicle) operating at high altitude with an underexpanded nozzle is shown here. The gas expands to vacuum isentropically, but the component of velocity to the sides (normal to the direction of rocket motion) contributes nothing to thrust, so it is effectively wasted. This is why, as we proved in Section 6.3.1, the rocket would achieve more thrust if the nozzle had a larger area ratio in order to more fully expand the flow so that the exit pressure more closely matched the ambient pressure.

If a rocket optimized for low ambient pressure is operated with a higher ambient pressure, the nozzle flow is *overexpanded*. In this case, the exit pressure is less than the ambient pressure, and an oblique shock wave will be forced into the exit flow. The oblique shocks from both sides of the nozzle lip will intersect in the center, setting up a complex series of shock and expansion interactions. If the nozzle is axisymmetric, the shocks will increase in strength as they focus in on the center of the exhaust flow, resulting in a Mach reflection. As the reflected shocks reach the interface between the exhaust gas and the ambient air, they will be reflected back into the exhaust flow as an expansion wave. These expansion waves interact and intersect the boundary again, now reflecting as a compression wave. This compression wave will steepen and coalesce into an oblique shock, setting up the pattern to repeat itself. The entire flow is quite complex and is beyond the scope of this treatment. These distinctive patterns of shock and expansion interactions in the nozzle exhaust are called *Mach diamonds* or *shock bottles*. This pattern can repeat itself over tens to hundreds of jet diameters. This pattern can be seen in the exhaust flow of jet engines, rocket engines, and even the exhaust of compressed air from a nozzle (e.g., shop air in a machine shop).

# 15. Method of Characteristics: Two-Dimensional Steady Flow

So far, we have only dealt with flows that are one-dimensional (Chapters 1-11) or are comprised of simple two-dimensional elements such as oblique shocks or Prandtl-Meyer expansion fans (Chapters 12-14). For more complex flows (say, over a curved wing or fuselage), it becomes necessary to develop new methodologies that can solve general two dimensional or multi-dimensional flows. One of the most versatile approaches is called the *method of characteristics*. It uses the fact that compressible flow is controlled by disturbances that propagate along waves or lines (also called characteristics or characteristic lines). These are not new concepts; we have already encountered the envelope of disturbances called the *Mach angle* in Section 4.3. As will be discussed in this chapter, the Mach line is a characteristic in steady, two-dimensional supersonic flow. By tracking how lines of influence propagate at the local Mach angle through a flow, it is possible to solve the entire flow field; this is the essence of the method of characteristics.

The method of characteristics is very general and very powerful. It can either be implemented on an *ad hoc* basis by hand or systemized into a computer-based algorithm. Implementing it for complex flows with shock waves, however, it can become cumbersome, and it has been largely replaced by finite-difference computational fluid dynamics (CFD) in recent decades. The method of characteristics is still worthy of our attention: examining characteristics is often essential to obtain a "feel" for how a flow responds to boundary conditions. In addition, the development of modern CFD codes is often built on an understanding of how characteristics control a compressible flow. Interestingly, some modern developments in CFD (such as space-time finite elements) are remarkably similar to the "classical" method of characteristics we will develop here.

## 15.1 Governing Equations for Irrotational Flow

In this Chapter, we will limit our attention to two-dimensional, steady supersonic flow. In addition, we will only consider irrotational flow. This is an important assumption, and it is worthwhile to detail what types of flow can, and cannot, be considered irrotational. An irrotational flow is a flow in which the vorticity of the flow is everywhere zero. Vorticity is defined as the curl of the velocity vector: vorticity = $\nabla \times \vec{V}$, where $\vec{V}$ is the velocity vector and $\nabla$ is the grad operator ($\hat{i}\frac{\partial}{\partial x} + \hat{j}\frac{\partial}{\partial y}$ for two-dimensional Cartesian coordinates). Swirling flows with eddies are obviously flows with vorticity. Some less obvious examples of rotational flow are flows in boundary layers or flows behind curved shock waves*; the version of the method of characteristics developed here will *not* be applicable to these flows. An example of an irrotational flow (where $\nabla \times \vec{V} = 0$ everywhere in the flow) includes an initially uniform flow passing through an isentropic converging-diverging nozzle.

The fact that the curl of velocity is everywhere zero in an irrotational flow means that the velocity vector $\vec{V}$ can be expressed in terms of a potential function $\phi$:

$$\vec{V} = \nabla\phi$$

Recall that a potential function is a scalar function whose gradient gives a vector field. It is a compact way of expressing the velocity vector field, and since it replaces the components of velocity with a single function, can lead to simplification in solving the flow. For example, the conservation of mass (continuity) for a steady flow:

$$\nabla \bullet (\rho\vec{V}) = 0$$

---

*It may not be obvious why flows with curved shock waves have vorticity. However, a powerful principle knows as Crocco's theorem, expressed as $\vec{V} \times (\nabla \times \vec{V}) = -T\nabla s$, explicitly links vorticity with a gradient in entropy. Since a curved shock wave in an initially uniform flow produces a gradient in entropy as the strength of the shock changes, the flow downstream of the shock must have non-zero vorticity. Implementing the method of characteristics for rotational flows (such as behind curved shocks) necessitates tracking an additional characteristic to account for the changing in entropy through the flow.

(note that this is simply the vector form of the conservation of mass derived in Section 2.1) can be written using the potential function as

$$\frac{\partial}{\partial x}(\rho u) + \frac{\partial}{\partial y}(\rho v) = \frac{\partial}{\partial x}(\rho \phi_x) + \frac{\partial}{\partial y}(\rho \phi_y) = 0$$

$$\rho(\phi_{xx} + \phi_{yy}) + \phi_x \frac{\partial \rho}{\partial x} + \phi_y \frac{\partial \rho}{\partial y} = 0 \tag{15.1}$$

We can eliminate $\rho$ (density) completely by invoking the momentum equation (recall Section 3.2):

$$\frac{dp}{\rho} + VdV = 0$$

or

$$dp = -\rho \frac{d(V^2)}{2} = -\rho \frac{d(\phi_x^2 + \phi_y^2)}{2} \tag{15.2}$$

If we further limit ourselves to isentropic flow, we can relate changes in density to changes in pressure by the definition of the speed of sound (recall Section 4.1):

$$c^2 = \left(\frac{\partial p}{\partial \rho}\right)_s$$

Thus, at any point in an isentropic flow:

$$d\rho = \frac{dp}{c^2}$$

Using (15.2) in this result, we obtain:

$$d\rho = -\frac{\rho}{c^2} d\left(\frac{\phi_x^2}{2} + \frac{\phi_y^2}{2}\right)$$

Thus, we can express the gradient of density in the *x*-direction as

$$\frac{\partial \rho}{\partial x} = -\frac{\rho}{c^2}\frac{\partial}{\partial x}\left(\frac{\phi_x^2 + \phi_y^2}{2}\right) = -\frac{\rho}{c^2}(\phi_x \phi_{xx} + \phi_y \phi_{yx})$$

and likewise for the *y*-direction:

$$\frac{\partial \rho}{\partial y} = -\frac{\rho}{c^2}\frac{\partial}{\partial y}\left(\frac{\phi_x^2 + \phi_y^2}{2}\right) = -\frac{\rho}{c^2}(\phi_x \phi_{xy} + \phi_y \phi_{yy})$$

We can use these expressions in (15.1) to eliminate density entirely:

$$\boxed{\left(1 - \frac{\phi_x^2}{c^2}\right)\phi_{xx} - \frac{2\phi_x \phi_y}{c^2}\phi_{xy} + \left(1 - \frac{\phi_y^2}{c^2}\right)\phi_{yy} = 0}$$

This relation is called the *velocity potential equation* and represents both the continuity and momentum equations for irrotational, isentropic flow. This equation is still coupled to the energy equation via the sound speed *c*. Since sound speed is a function of temperature, it will be necessary to solve for temperature using the energy equation.

## 15.2 Properties of Hyperbolic Systems: Characteristics

We will re-introduce the velocity components *u* and *v* for a moment to make a few points:

$$\left(1 - \frac{u^2}{c^2}\right)\phi_{xx} - \frac{2uv}{c^2}\phi_{xy} + \left(1 - \frac{v^2}{c^2}\right)\phi_{yy} = 0 \tag{15.3}$$

Thus, compressible flow is governed by a PDE of the form:

$$A\frac{\partial^2\phi}{\partial x^2} + 2B\frac{\partial^2\phi}{\partial x\partial y} + C\frac{\partial^2\phi}{\partial y^2} = 0$$

where $A = 1 - \frac{u^2}{c^2}$, $B = -\frac{uv}{c^2}$, and $C = 1 - \frac{v^2}{c^2}$. From the basic theory of partial differential equations, PDE's of this form can be classified as follows:

$$B^2 - AC < 0 \Rightarrow \text{elliptic}$$

$$B^2 - AC = 0 \Rightarrow \text{parabolic}$$

$$B^2 - AC > 0 \Rightarrow \text{hyperbolic}$$

The canonical *elliptic* PDE is the Laplace equation: it is governed by smooth solutions where all boundary conditions have an influence on the solution at every point in the domain (think of the steady state temperature distribution in a plate with temperature prescribed along the edges). The classic example of a *parabolic* equation is the heat (or diffusion) equation: in parabolic systems, initial conditions simply spread or diffuse outward over time, but the influence of a source is felt instantaneously throughout the domain (think of temperature diffusing outward into a rod after being given an initial heat pulse at one end). The most familiar example of a *hyperbolic* equation is the wave equation ($\frac{\partial^2\phi}{\partial t^2} - c^2\frac{\partial^2\phi}{\partial x^2} = 0$), where information propagates via waves that move at a specific speed. With a hyperbolic system, a source or disturbance has a clearly defined zone of influence (return to the picture of throwing rocks into a pond or river, as discussed in Section 4.3).

For steady, irrotational flow, the quantity $B^2 - AC$ can be shown to equal

$$B^2 - AC = \frac{u^2 + v^2}{c^2} - 1 = \frac{V^2}{c^2} - 1 = M^2 - 1$$

Thus, the type of PDE governing a flow changes as the flow goes from subsonic to supersonic. *Subsonic flow* is governed by an elliptic PDE: since the flow is everywhere subsonic, the influence of upstream and downstream conditions can be felt everywhere in the flow, and the solution is able to accommodate smoothly. In fact, in the limit as $V << c$ (incompressible limit), the potential equation reverts to the Laplace equation ($\frac{\partial^2\phi}{\partial x^2} + \frac{\partial^2\phi}{\partial y^2} = 0$). In *supersonic flow*, the effect of a boundary or source is only felt in a domain of influence that is defined by the speed at which information propagates. The fact that every point in the solution cannot communicate to everywhere else in the domain can give rise to discontinuous jumps (shock waves).

Hyperbolic partial differential equations in general have a unique feature. Along certain lines, called characteristics, the partial differentials become undefined (or, more properly, *indeterminate*). Along these lines the PDE may "collapse" to simpler ordinary differential equations or even algebraic equations. You are encouraged to consult a text book on partial differential equations for a full development; the development here will only give you a taste of the idea. For example, suppose we solve (15.3) for $\frac{\partial v}{\partial y}$:

$$\frac{\partial v}{\partial y} = \phi_{yy} = \frac{\frac{2uv}{c^2}\frac{\partial v}{\partial x} - \left(1 - \frac{u^2}{c^2}\right)\frac{\partial u}{\partial x}}{\left(1 - \frac{v^2}{c^2}\right)} \tag{15.4}$$

Thus, $\frac{\partial v}{\partial y}$ is known as a function of how $u$ and $v$ vary along the $x$-direction ($\frac{\partial u}{\partial x}$ and $\frac{\partial v}{\partial x}$). This partial derivative will be indeterminate, however, when $v = c$ (denominator goes to zero). Consider a point in the flow where this happens. The angle the flow makes with the horizontal is:

$$\theta = \sin\frac{c}{V} = \sin\frac{1}{M} = \alpha$$

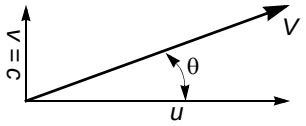


Thus, when the angle of the flow with respect to the horizontal becomes equal to the Mach angle, the partial derivative of the *v*-velocity component in the *y*-direction becomes undefined. The only way the expression (15.4) can avoid "blowing up" in this case is if the numerator is also zero, and the expression is indeterminate. Setting the denominator of (15.4) equal to zero, we obtain the *compatibility equation*:

$$\frac{2uv}{c^2}\frac{\partial v}{\partial x} - \left(1 - \frac{u^2}{c^2}\right)\frac{\partial u}{\partial x} = 0 \text{ along the } x\text{-direction.}$$

This equation is really an ordinary differential equation, and we should replace $\frac{\partial}{\partial x}$ with $\frac{\mathrm{d}}{\mathrm{d}x}$, since it is only dependent on how properties vary in a single direction (the *x*-direction). The horizontal line in this case becomes a *characteristic*.

Note that the orientation of the *x* and *y* axes is arbitrary; we can always rotate the axes to find an orientation where one axis will be at the Mach angle with respect to the flow. *Thus, any line that is at the Mach angle* $\alpha$ *with respect to the flow is a characteristic.*

The formal technique to find the characteristics of a system is to express the system as algebraic linear equations:

$$A\frac{\partial^2\phi}{\partial x^2} + 2B\frac{\partial^2\phi}{\partial x\partial y} + C\frac{\partial^2\phi}{\partial y^2} = 0$$

$$dx\left(\frac{\partial u}{\partial x}\right) + dy\left(\frac{\partial u}{\partial y}\right) + 0\left(\frac{\partial v}{\partial y}\right) = du$$

$$0\left(\frac{\partial u}{\partial x}\right) + dx\left(\frac{\partial u}{\partial y}\right) + dy\left(\frac{\partial v}{\partial y}\right) = dv$$

Solving for $\frac{\partial u}{\partial x}$ using the techniques of linear algebra (Cramer's rule):

$$\frac{\partial u}{\partial x} = \frac{\begin{vmatrix} 0 & 2B & C \\ du & dy & 0 \\ dv & dx & dy \end{vmatrix}}{\begin{vmatrix} A & 2B & C \\ dx & dy & 0 \\ 0 & dx & dy \end{vmatrix}} = \frac{-du(2Bdy - Cdx) - dvCdy}{Ady dy - dx(2Bdy - Cdx)} \tag{15.5}$$

And likewise for $\frac{\partial u}{\partial y}$ and $\frac{\partial v}{\partial y}$. Setting the denominator equal to zero gives a quadratic equation for $\frac{\mathrm{d}y}{\mathrm{d}x}$:

$$\left(\frac{\mathrm{d}y}{\mathrm{d}x}\right)_{\text{char}} = \frac{B \pm \sqrt{B^2 - AC}}{A} = \frac{-\frac{uv}{c^2} \pm \sqrt{\frac{u^2 + v^2}{c^2} - 1}}{1 - \frac{u^2}{c^2}}$$

Thus, there are two different lines along which the partial derivative becomes indeterminate, this expression gives the slope of these lines. Introducing $u = V\cos\theta$ and $v = V\sin\theta$ and $\alpha = \sin^{-1}\frac{1}{M} = \sin^{-1}\frac{c}{V}$:

$$\left(\frac{\mathrm{d}y}{\mathrm{d}x}\right)_{\text{char}} = \frac{-\frac{\cos\theta\sin\theta}{\sin^2\alpha} \pm \sqrt{\frac{\cos^2\theta + \sin^2\theta}{\sin^2\alpha} - 1}}{1 - \frac{\cos^2\theta}{\sin^2\alpha}}$$

Note that $\sqrt{\frac{\cos^2\theta + \sin^2\theta}{\sin^2\alpha} - 1} = \frac{1}{\tan\alpha}$, so this expression simplifies to:

$$\left(\frac{\mathrm{d}y}{\mathrm{d}x}\right)_{\text{char}} = \tan(\theta \mp \alpha)$$

The graphical interpretation of this result is shown here:

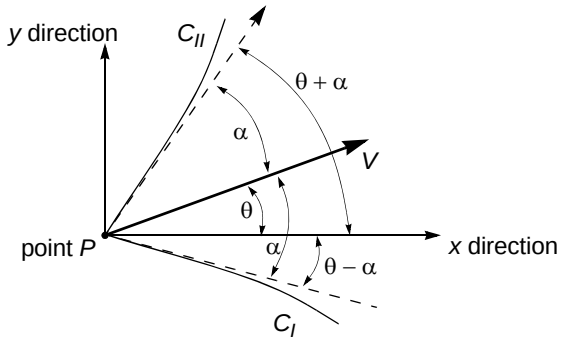


Note than the expression $\left(\frac{dy}{dx}\right)_{char} = \tan(\theta \mp \alpha)$ gives the slope of a line that is oriented at the Mach angle $-\alpha$ (or $\alpha$) with respect to the flow direction. We have encountered these lines before: they are *Mach lines* (see Section 4.3). We now see that Mach lines are also characteristics. We will denote the two Mach lines as the *right-running characteristic* and the *left-running characteristic* ($C_I$ and $C_{II}$, respectively). These names derive from the fact that if we disturb the flow at point $P$ (imagine, dipping a finger into the flow), would see one Mach line running off toward the right and another toward the left. In the sketch here, the characteristics are shown to curve, because they may be moving into a region of flow where $\theta$ and $\alpha$ are changing. But locally (at the point $P$), their slopes are given by $\tan(\theta \mp \alpha)$.

We now turn to the numerator of (15.5), its value must also be zero in order to keep the flow field derivatives from blowing up:

$$\frac{dv}{du} = \frac{dx}{dy} - \frac{2B}{C}$$

Using the fact that this condition will only apply along the characteristics, where we know $\frac{dy}{dx} = \left(\frac{dy}{dx}\right)_{char}$, we can obtain (note: many steps of algebra skipped over):

$$\frac{dv}{du} = \frac{\frac{uv}{c^2} \mp \sqrt{\frac{u^2+v^2}{c^2} - 1}}{1 - \frac{v^2}{c^2}}$$

Using $u = V\cos\theta$ and $v = V\sin\theta$ and considerable manipulation, we obtain:

$$d\theta = \mp\sqrt{M^2 - 1}\frac{dV}{V}$$

This is our compatibility equation, where the "–" sign applies along $C_I$ characteristics and the "+" sign applies along $C_{II}$ characteristics. This is an ordinary differential equation, which we can now integrate. Looking back to Section 13.1, however, we note that we already integrated this relation: when integrated, it yields the *Prandtl-Meyer Function*: $\nu(M)$. Thus, our compatibility conditions become algebraic equations:

$C_I = \nu(M) + \theta$ = constant along right-running characteristics

$C_{II} = \nu(M) - \theta$ = constant along left-running characteristics

Thus, the quantities $C_I$ and $C_{II}$ are constant along right-running and left-running characteristic, respectively. This concept takes some getting used to, but is very powerful: imagine a point in a supersonic flow that generates a tiny disturbance. The disturbance will propagate out from that point along Mach lines (one to the right, one to the left), and they carry a piece of information along with them. That information is that the quantity $C_I = \nu(M) + \theta$ is a constant (or $C_{II} = \nu(M) - \theta$ is a constant). As this disturbance propagates through the flow, it will encounter regions with different flow angle $\theta$ and different Mach number $M$. The sum of $\nu(M) + \theta$, however, *will always remain a constant* (provided the flow remains supersonic and irrotational). This remarkable property permits us to solve an entire supersonic flowfield, provided we know the conditions entering the flow boundary.

## 15.3 Solution Techniques

### 15.3.1 Solving for a Point in the Flow

Let us assume that there are two points in a supersonic flow at which we have complete knowledge of the flow: Points 1 and 2. At Point 1, the flow is moving upward and to the right with flow angle $\theta = 20°$ at Mach 2. At Point 2, the flow is less inclined ($\theta = 5°$) but moving a bit faster ($M = 2.1$). We will also assume we know the exact $(x,y)$ coordinates of each point.

We can imagine that there is an infinitesimal disturbance emanating from Point 1, that sends characteristic Mach lines streaming off to the left and right. Since we know $\theta$ and Mach number at Point 1, we know the value of $C_I$ and $C_{II}$ these characteristics carry with them: $(C_I)_1 = 26.38° + 20° = 46.38°$ and $(C_{II})_1 = 26.38° - 20° = 6.38°$. Likewise, Point 2 has two characteristics streaming away from it as well: $(C_I)_2$ and $(C_{II})_2$.

At some point in the flow, the right running characteristic from Point 1 $(C_I)_1$ and the left running characteristic from Point 2 $(C_{II})_2$ will intersect. Note that we can approximately locate this point in the flow by making a geometric construction (i.e., straight edge and protractor): we know the right running and left running characteristics have angles $\theta + \alpha$ and $\theta - \alpha$ with respect to the horizontal. While the characteristic may curve as they move through regions of nonuniform flow, we can locally approximate them as straight lines.

Note that while we do not know *a priori* what the flow properties are at Point 3, we do know that $(C_I)_1 = 46.38°$ and $(C_{II})_2 = 24.07°$. Both these values must apply at Point 3. Using this information, we can solve for $\theta_3$ and $\nu_3$:

$$\theta = \frac{C_I - C_{II}}{2} \qquad \nu = \frac{C_I + C_{II}}{2}$$

$$\theta_3 = \frac{46.38° - 24.07°}{2} = 11.15° \qquad \nu_3 = \frac{46.38° + 24.07°}{2} = 35.22°$$

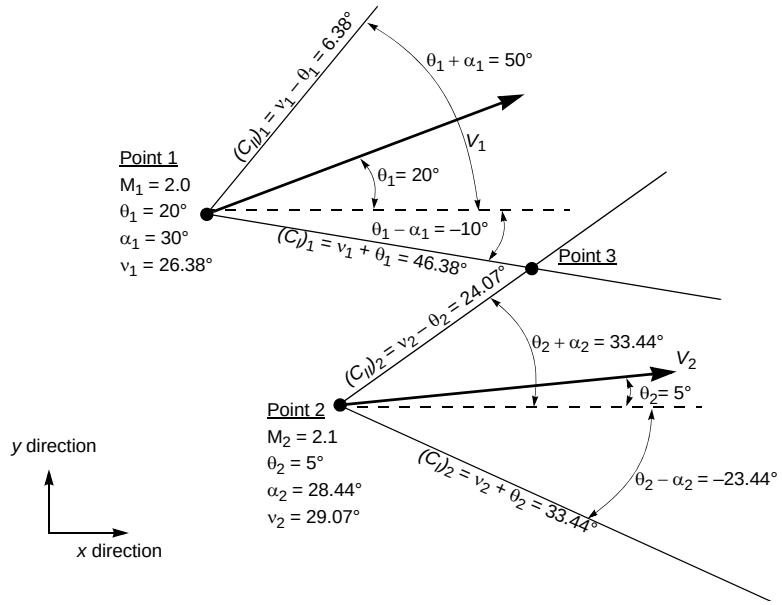


Knowing $\nu_3$, we can find Mach number using a table of Prandtl-Meyer function values: $M_3 = 2.34$. Thus, we can completely solve for the conditions at Point 3 (pressure, temperature, etc. can be found using isentropic relations, assuming we know the stagnation temperature and pressure of the flow).

Now that we know the values of $\theta$ and $\alpha$ at Point 3 ($\theta_3 = 11.15$, $\alpha_3 = 25.30°$), we could revise the geometric construction we used to find the $(x,y)$ location of Point 3 (i.e., get out protractor and straight edge again) by using the average values of the flow and Mach angles:

$$\theta_{13} = \frac{1}{2}(\theta_1 + \theta_3) = 15.58°, \text{ etc. for } \theta_{23}, \alpha_{13}, \alpha_{23}$$

since these values are more representative of the actual flow the characteristics propagate through. Thus, we can improve the accuracy of our solution.* Note that the values of the flow properties at Point 3 do not change as we do this iteration, only the location of Point 3 changes.

Note that the Mach number at Point 3 is greater than at Points 1 and 2. This agrees with the intuition we developed in studying one-dimensional flow: since the flow is supersonic and diverging, it should accelerate and Mach number should increase.

Also note that the characteristics do not terminate at Point 3, they continue on through the flow, carrying their information about $C_I$ and $C_{II}$ with them. Alternative, we can imagine that new $C_I$ and $C_{II}$ characteristics emanate from Point 3; their values of $(C_I)_3$ and $(C_{II})_3$ will be the same as $(C_I)_1$ and $(C_{II})_2$. When they intersect characteristics of another type (e.g., a right running characteristic intersects a left running characteristic), we can solve for that new point in the flow via the same technique.

### 15.3.2 Solving for a Point on the Wall

Let us return to the $C_I$ characteristic that emanated from Point 1. Let us assume that this characteristic eventually encounters a wall. Again, we can estimate the point of this intersection with the wall via a geometric construction, assuming the characteristic remains at a constant angle $\theta_1 + \alpha_1$. Where it hits the wall at Point 4, value of $(C_{II})_1$ must still apply. We do not have the $C_I$ characteristic at the point, but since the flow must be parallel to the wall, we do have a value of $\theta$ (say, $\theta_{wall} = \theta_4 = 13°$). Thus, we can solve for $\nu_4$ and Mach number:

$$\nu_4 = (C_{II})_1 + \theta_4 = 19.38°$$

So, $M_4 = 1.75$, from a look-up of Prandtl-Meyer function values. Thus, we now have complete knowledge about this point on the wall, including the value of $(C_I)_4$ for a new right-running characteristic that is emanated from this point.

*In practice, it is often not worth correcting the position of the new point using the average values. In a numerical solution, it is often easier to just add more characteristics, thus shortening the distance over which they need to travel before solving for the next point and thereby decreasing the error. By continuing to increase the number of characteristics, you can quickly converge to a final solution.

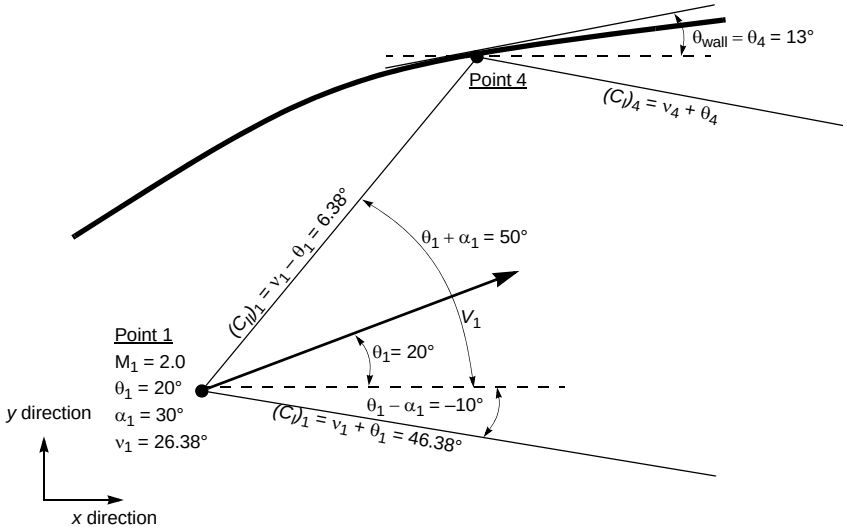


## 15.4 Solving a Complete Flowfield

By combining the point-wise solution techniques developed above, we can now march through a supersonic flow and solve for each point where characteristics intersect. This requires that we have complete knowledge of the flow along some line (*not* a characteristic line). Typically, this is an upstream boundary where the flow enters the domain of interest. For a nozzle, for example, we would need to know the flow conditions at some line or plane downstream of the throat. Note that we cannot initialize our characteristic solution with the sonic flow at the throat, since the method of characteristics breaks down for sonic flow. We need to initialize the solution with a supersonic flow (say, Mach 1.1).

Once we have an upstream boundary specified, we can start streaming characteristics downstream from points on the boundary. Where the characteristics intersect, we can solve for the flow conditions at that point. If the characteristics intersect the wall, we will know the wall angle and thus can

solve for the flow there, and stream new characteristics back into the solution domain.

Constructing a table of flow variables and characteristics is often essential to successfully implement the method. This is illustrated in the numerical example below.

### 15.5.1 Numerical Example: Supersonic Flow into a Converging Channel

Consider supersonic flow entering a channel that has converging walls of fixed angle 10°. The flow enters at Mach 3, and is parallel to the wall at the wall and runs horizontal at the center line of the channel. Using the method of characteristics, solve for the flow as it continues down the channel.

We will initialize our solution by choosing three points on the boundary that was specified (the inlet plane of the channel): Points 1, 2, and 3. Since we have complete knowledge about these points, we can determine the values of $C_I$ and $C_{II}$ and stream those values into the flow. For example, the $C_I$ characteristic from Point 1 intersects the $C_{II}$ characteristic from Point 2 at Point 4. Knowing $C_I$ and $C_{II}$, we solve for Point 4, and then stream characteristics on from Point 4 to Points 6 and 7.

In the table shown here, values that are known *a priori* either from the initial boundary or the wall are denoted with a heavy box. Values that are obtained by streaming characteristics from known values are denoted with a double-lined box. Once any two of the four parameters ($C_I$, $C_{II}$, $\nu$, $\theta$) is known, the other two are automatically determined, and then the Mach number and other flow parameters (Mach angle, etc.) can be solved for. These other values are listed in the table ($M$, $\theta$, $\theta+\alpha$, and $\theta-\alpha$), but note that they are not required to solve for the values of $C_I$, $C_{II}$, $\nu$, or $\theta$. They *are* used in performing the graphical construction to determine where the points will lie in physical space. We have stopped at Point 7, but the method can be extended further.

Note that solving for the lower half of the channel was redundant. Since the channel was symmetric, we could have replaced the center line with a horizontal wall and the solution would have remained the same. If we wish to increase the accuracy of our solution, we can increase the number of initial characteristics emitted from the initial datum line. For example, we can introduce a point halfway between Points 1 and 2.

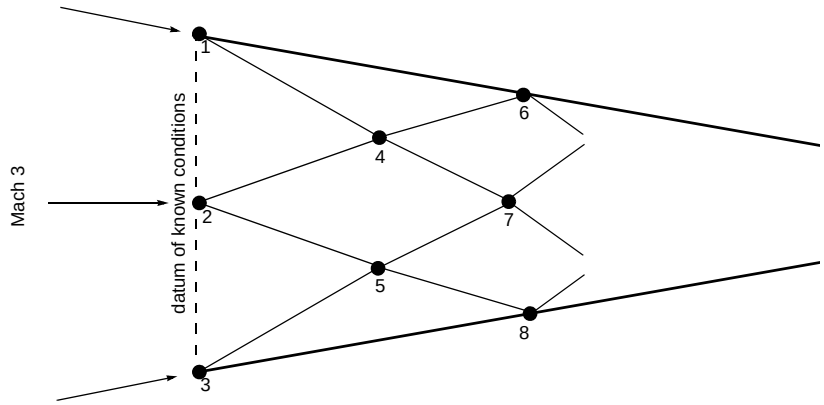


| Point | $C_I$ | $C_{II}$ | $\theta$ | $\nu$ | $M$ | $\alpha$ | $\theta+\alpha$ | $\theta-\alpha$ |
|---|---|---|---|---|---|---|---|---|
| 1 | 39.757° | 59.757° | -10° | 49.757° | 3.00 | 19.47° | 9.47° | -29.47° |
| 2 | 49.757° | 49.757° | 0° | 49.757° | 3.00 | 19.47° | 19.47° | -19.47° |
| 3 | 59.757° | 39.757° | 10° | 49.757° | 3.00 | 19.47° | 29.47° | -9.49° |
| 4 | 39.757° | 49.757° | -5° | 44.757° | 2.753 | 21.3° | 16.3° | -26.3° |
| 5 | 49.757° | 39.757° | 5° | 44.757° | 2.753 | 21.3° | 26.3° | -16.3° |
| 6 | 27.755° | 49.757° | -10° | 39.757° | 2.527 | 23.31° | 13.31° | -33.31° |
| 7 | 39.757° | 39.757° | | | | | | |

## 15.6 Breakdown of the Method

The solution above can be continued until one of two things happen:

- *Characteristics running in the same direction cross.*
- *The flow becomes subsonic.*

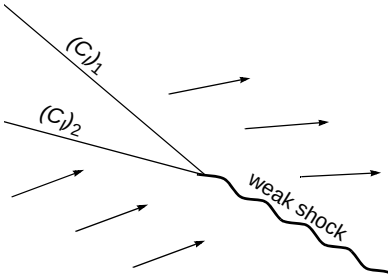


"Characteristics running in the same direction" means, for example, two $C_I$ characteristics, streaming from different points in space, intersect, as shown here. When this happens, technically the two waves merge to form a stronger, finite amplitude wave that can no longer be considered a characteristic; it has become a *shock wave* (albeit a weak one). If you review Chapter 13, this is exactly how we discussed oblique shock waves forming on a smoothly curved corner: Mach lines (or characteristics) intersect and coalesce to form an oblique shock. Once a shock wave appears, our flow is no longer isentropic or irrotational, the key assumptions upon which our method was developed. If the shock wave generated is weak, it may be possible to "get away with" continuing to treat it as a characteristic, although the fact that two characteristics have now become one can wreak havoc on our bookkeeping system (or computerized algorithm). If characteristics continue to merge, the oblique shock gets stronger, and we really cannot justify continuing the solution. There are ways the method of characteristics can be modified to handle these situations, but finite difference CFD codes are typically much better in these cases.

The other thing that will cause our solution method to break down is the appearance of sonic (or subsonic) flow. Again, there are ways that the method of characteristics can be modified to handle interacting with regions of subsonic flow (although the method itself cannot apply in those regions).

## 15.7 Some Comments

As one is implementing the method of characteristics, the operation using the information propagated along characteristics to solve for the flow at a new point where characteristics interact becomes routine, consisting of simple addition and subtraction and table look-ups of $\nu(M)$ and $\alpha(M)$. The main challenge becomes careful bookkeeping of the characteristic information. As simple as these operations are, one should not lose sight of the fact that, in implementing the method of characteristics, *you are actually solving a coupled set of nonlinear partial differential equations*! This is no small feat, since in general, solving nonlinear PDE's is a task that demands considerable mathematical prowess or serious computational power.

Another thought to keep in mind in implementing the method of characteristics is that, to some degree, this is how Nature itself "solves" a compressible flow. In actuality, there are an infinite number of characteristics in a real, physical domain of flow: they form a continuum. In the method of characteristics, these are approximated by a finite number of characteristics. In laboratory experiments, the trajectory of a few characteristics can be observed by, for example, making scratches on the walls of a channel to induce a finite (but still very weak) disturbance that can be visualized by techniques such as Schlieren. This has been done in the photograph shown here, where grooves that have been scratched into the walls of a wind tunnel permit the characteristics to be visualized. *Characteristics are real.* (The zebra-patterns here are not related to characteristics; they are a result of a flow visualization technique called interferometry that permits us to visualize density contours in a flow.)

Finally, if the development of the method of characteristics seems so mathematical as to be opaque, then you might look forward to Chapter 16, where the method is developed for one-dimensional unsteady flow. In one-

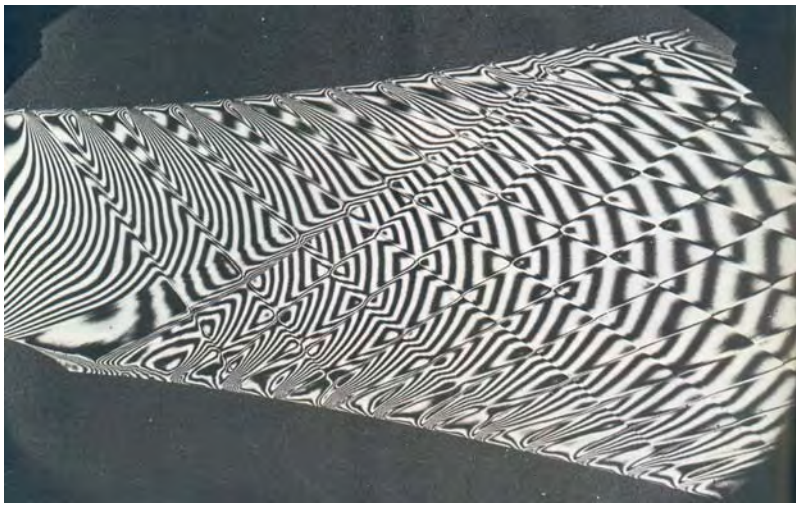

Taken from M. van Dyke, *An Album of Fluid Motion*, Parabolic Press, Stanford, California, 1982. Originally from Hiller & Meier (1975).

dimensional unsteady flow, the characteristics again turn out to be acoustic waves, but the characteristics and compatibility conditions can be derived in a more transparent and intuitive fashion.

## 15.8 Examples of Applying the Method of Characteristics*

The method of characteristics can be implemented in a computer program such that a large number of characteristics can be tracked. This has been done using Matlab, and the results for an initially slightly supersonic flow ($M_{in}$ = 1.000001) entering a channel with an upper wall that diverges at a constant angle of 20° are shown below. The method of characteristics solution was initialized with a Prandtl Meyer expansion fan at the corner: knowing the Prandtl-Meyer flow, a finite number of characteristics were specified. The characteristics then reflected off the lower wall and proceeded to "bounce" back and forth between the two walls, with each interaction between characteristics being solved via the methods outlined above.

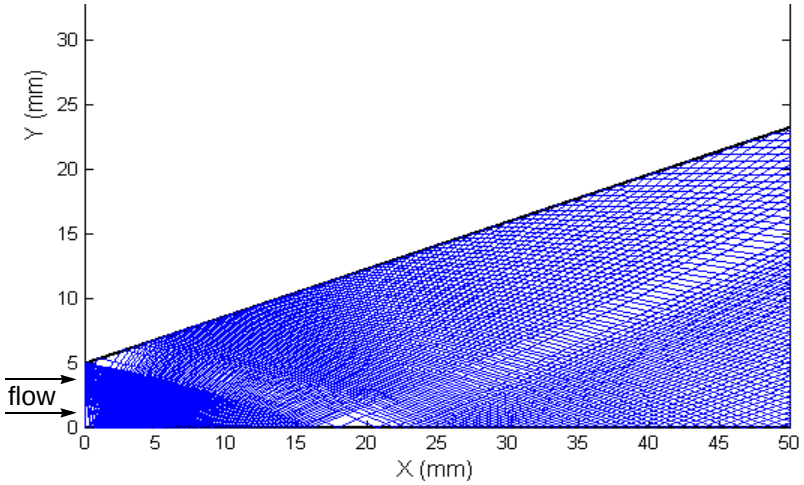


*Calculations in this section performed by Patricia Vu, McGill University.

It is interesting to see how this two-dimensional solution compares with the one-dimensional solution to isentropic flow in a diverging channel developed in Chapter 5. This comparison is made below, in which the Mach number of the flow at each characteristic intersections is plotted as a function of the area at that cross section (normalized by the inlet area where the flow is sonic). This forms a dense "cloud" of points, since there are a large number of characteristics being used. The solid line is the $\frac{A}{A^*}$ relation for one-dimensional flow from Chapter 5. Note the excellent agreement between the two solutions. The agreement can be made even better if the channel area is modified to vary more slowly. This result is a good validation of the method of characteristics solver (or a good validation of one-dimensional flow, depending on your perspective).

A method of characteristics program such as this can be used to solve more complex problems where one dimensional solutions are not available, such as the supersonic flow over a curved wedge. A solution to the hypersonic flow ($M$ = 17.7) over a curved wedge whose surface is described by a power law ($y = 0.2\ x^{0.8}$) using the same program is shown below. Note that, due to the

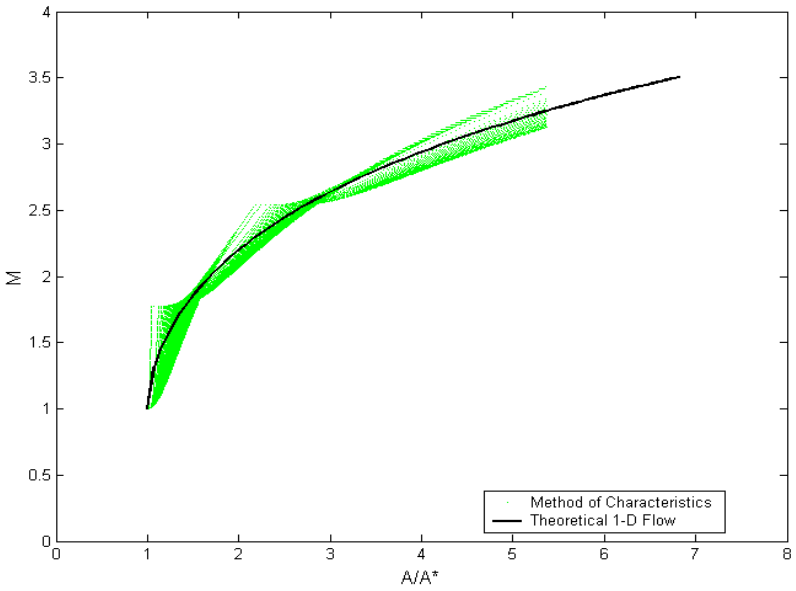

curved shock wave, the flow is no longer irrotational. Thus, the solver needed to track an additional characteristic (the particle paths) in order to account for the nonuniform entropy of the flow. This required a minor modification to the solution techniques developed in this chapter.